Journal of Statistical Physics, Vol. 48, Nos. 3/4, 1987

A Cell Dynamical System Model of Chemical Turbulence

Y. Oono[1] and C. Yeung[1]

Received December 30, 1986

A cellular-automaton-like caricature of chemical turbulence on an infinite one-dimensional lattice is studied. The model exhibits apparently "turbulent" space-time patterns. To make this statement precise, the following problems or points are discussed: (1) The infinite-system-size limit of such cell-dynamical systems and its observability is defined. (2) It is proved that the invariant state in the large-system-size limit of the "turbulent" phase exhibits spatial patterns governed by a Gibbs random field. (3) Potential characteristics of "turbulent" space-time patterns are critically surveyed and a working definition of (weak) turbulence is proposed. (4) It is proved that the invariant state of the 'turbulent" phase is actually (weak) turbulent. Furthermore, we conjecture that the turbulent phase of our model is an example of a K system that is not Bernoulli.

KEY WORDS: Chemical turbulence; cellular automaton; dynamical systems.

1. INTRODUCTION

Many systems with interesting phenomena such as pattern formation, turbulence, etc., have not only temporal, but spatial structures. The recent revival of interest in the collective behavior of coupled simple subsystems such as cellular automata (CA)[1,2] and coupled maps (CM)[3] stems from the quest for the role of spatial degrees of freedom.

In the present paper we analyze in detail our caricature model of chemical turbulence,[4] which is a kind of cellular automaton without a quiescent state. We first discuss the infinite-system-size limit of cellular-automaton-like systems and its empirical accessibility (observability), and

[1] Department of Physics and Material Research Laboratory, University of Illinois at Urbana-Champaign, Urbana, Illinois 61801.

0022-4715/87/0800-0593$05.00/0

deduce the macroscopic phase diagram for our model from the microscopic mechanics (i.e., local rules). Our caricature model exhibits an apparently "turbulent" phase, which we call the T-phase. In the T-phase we show that, in the infinite-system-size limit, there is a unique observable stationary state whose spatial structure is described by a Gibbs random field (e.g., Ref. 5). Next, we discuss how to characterize at least weakly turbulent space-time patterns and propose a working definition. We then prove that the T-phase of our model is actually weakly turbulent.

The problem of fluid turbulence and the theory of dynamical systems were connected by Ruelle and Takens.[6] The study of systems with a few degrees of freedom has attracted much attention since the enlightening paper by McLaughlin and Martin,[7] which popularized the highly original paper by Lorenz[8] as well as the work of Ruelle and Takens. Much simpler systems, such as maps of an interval to itself, also have attracted researchers, especially after the papers by Li and Yorke[9] and May.[10] So far no special attention has been paid to the spatial structure (if any) of dynamical systems; even partial differential equations (PDE) have been considered as ordinary differential equations in certain function spaces. The only exception may be the studies of Liapunov characteristic number density, etc., of PDEs by Ruelle and others.[11] On the other hand, numerical experiments on PDE, coupled maps, and CA have become increasingly popular among researchers in physics and other fields. In these studies spatial patterns or space-time patterns such as intermittency have been considered interesting.[12] Therefore, the points of view of the ordinary theory of dynamical systems and of the main interest of numerical experimentalists have been more or less orthogonal. Since one of the most interesting problems in the theory of dynamical systems is the study of the long-time behavior of the systems, to obtain a dynamical-system-theoretic framework of CA, we should study infinitely big lattice systems. Only on such a lattice can we unambiguously discuss entropies, the Liapunov characteristic numbers, and other dynamical quantities. However, we obviously cannot study or observe infinite lattice systems empirically. Therefore, strictly speaking, interesting states of infinitely big lattice systems are those that we can somehow reach by some limiting procedure from observations of finite systems. We will discuss a definition of the large-size limit and its observability.

One of the conceptual issues in the study of maps is the characterization of chaos. We believe that the issue has been settled. For example, one definition due to Oono[13] for an endomorphism $T: \tilde{\Omega} \to \tilde{\Omega}$ of a set $\tilde{\Omega}$ is as follows: we say that T exhibits (formal) chaos if and only if there exists, for a positive integer m, a T^m invariant subset $\tilde{\Omega}_1 \subset \tilde{\Omega}$, and a one-to-one map Φ so that the diagram in Fig. 1 becomes commutative, where

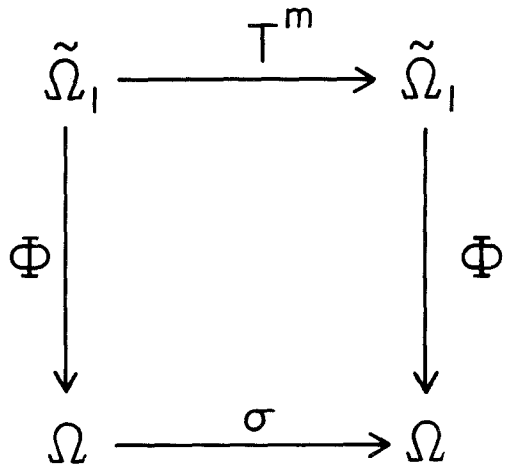

Fig. 1. A definition of chaos. $\tilde{\Omega}_1$ is a T^m-invariant set of the system $T: \tilde{\Omega} \to \tilde{\Omega}$, where m is a positive integer and $\tilde{\Omega}_1 \subset \tilde{\Omega}$, $\Omega = \{0, 1\}^N$, the set of all the semi-infinite sequences consisting of 0 and 1, and σ is the full shift on Ω, i.e., $\sigma: \Omega \to \Omega$ is the coin tossing process. If we find a bijection ϕ such that this diagram is commutative, we say $T: \tilde{\Omega} \to \tilde{\Omega}$ exhibits chaos.

$\Omega = \{0, 1\}^N$ (henceforth N denotes the set of all the positive integers) is the set of all semi-infinite sequences of 0 and 1 and σ is the full shift. In more informal words, if we can find a nice relation between a dynamical system and a stochastic process (say, the coin tossing process), we say that the system exhibits chaos. The nicety of this definition has been well demonstrated.[14] Notice that the definition automatically implies the sensitivity of the system to initial conditions stressed by Guckenheimer[15] and others. The relation of this definition to algorithmic randomness[16] is obvious, and has been noted and stressed.[2] Simultaneously, Ford[17] also advocated a similar definition of chaos. Brudno's celebrated theorem[18] relating the algorithmic complexity of trajectories and the Kolmogorov–Sinai entropy is the theoretical basis of our point of view. On the other hand, the concept "turbulence" should be more specific than chaos. "Turbulent" dynamical systems must be chaotic, but the converse should not hold: who would call a spatially homogeneous but temporally chaotic system a turbulent system? Thus, in order to characterize "turbulence," we must respect spatial patterns exhibited by the system. As far as we know there have been no serious attempts in this direction except for preliminary analyses by Wolfram[19] and Packard.[20]

We believe that the essence of turbulent space-time patterns lies in the

[2] Y. Oono and Y. Takahashi, invited talks in Japan at various meetings on chaos, 1979.

incompatibility between two choices of partitionings of the state space A^L; one is a partition based on the visual similarity of spatial patterns and the other is the partition generated by a generator of dynamics (or more intuitively, based on similarity of fates of patterns). If these two choices are incompatible, each component of one partition overlaps many components of the other. In this paper we try to quantify this incompatibility, and give a working definition of weak turbulence. We, however, hesitate to call any pattern produced by CA turbulent in the genuine sense, because, as we will see, the Kolmogorov–Sinai entropy for the observable (i.e., empirically accessible) measure is finite even in the infinite-lattice-size system. Therefore we introduce a weaker concept to discuss apparently complicated patterns.

We occasionally pay attention to coupled maps also. It is convenient to define a class of dynamical systems which includes both CA and CM: *cell dynamical systems* (CDS). A CDS is an endomorphism $T: A^L \to A^L$, where A is a set and L is a lattice (in the physicists' sense, e.g., d-cubic lattice Z^d, Z being the set of all integers, as usual). The present paper should be regarded as part of a more general study of CDS.

There are two main aims in the general study of CDS: [A] to study CDS as models of nonequilibrium phenomena; [B] to use CDS to understand fundamental conceptual issues. Aim [A] consists of [Aa] construction of simple but nontrivial models of real phenomena such as fluid turbulence and [Ab] use of resultant models to explore principles of nonequilibrium statistical physics. Aim [B] consists of [Ba] construction of a theoretical framework for dynamical systems that have nontrivial space-time structures, and [Bb] use of CDS to understand conceptual questions such as, "What is the randomness of space-time patterns?" There are many studies in [Aa]; typical examples are cellular automaton hydrodynamics[21] and coupled-map models of spinodal decomposition.[22] However, there seems to be no study in the category [Ab]. This will include the application of thermodynamic framework for chaos[5,23] to CDS. Dynamical-system-theoretic studies of CA are not new. There exist ergodic theoretical studies[24,25] for restricted classes of CA. However, even very fundamental questions have yet to be discussed. For example, the large-system-size limit (the counterpart of the thermodynamic limit in ordinary equilibrium statistical mechanics) of CDS has not been considered. Preliminary studies[19,20] exist in the category [Bb].

Since the present paper is rather lengthy, we here give a roadmap and the main conclusions of each section. We use Walters[26] as the standard source of definitions of mathematical terminology thoughout the paper.

In Section 2 chemical turbulence is explained. This section summarizes theoretical and experimental background. An empirically obtained phase

diagram for the Belousov–Zhabotinsky reaction is reproduced here for convenience.

In Section 3 chemical turbulence is modeled as a CA that does not have a quiescent phase, and empirical results obtained from simulations are summarized. We show that there are three nontrivial phases T, S_a, and S_b; T is the "turbulent" phase, and S_a, S_b are phases with solitons (or kinks).

In Section 4 the "thermodynamic limit" (large-lattice-size limit) of CA and its observability is defined. All the technical details are given in the Appendix. With this preparation we can safely and meaningfully talk about entropies of the CA, which are obtainable from the observation of finite systems. Simple examples that will be used later as counterexamples are briefly discussed.

Sections 5 and 6 discuss the nontrivial phases (stationary states) of our chemical turbulence model. In Section 5 observed macroscopic behaviors on finite lattices are rigorously deduced from the microscopic dynamics (i.e., the local CA rules). In Section 6 the infinite-system-size limit of these phases are discussed. In this limit the phases S_a and S_b are shown to be spatially homogeneous and the T-phase exhibits an observable stationary state characterized by a Gibbs random field. Since a large part of these two sections is highly technical, each section starts with an outline and a summary, so that the reader can skip the technical details completely without much difficulty in following the rest of the discussion.

In Section 7 we survey possible characterizations of turbulent space-time patterns. We conclude that entropies, complexity, etc., are not adequate characteristics of "turbulence."

Then in Section 8 we propose a definition of "weak turbulence" and prove that the T-phase of our model is actually weak-turbulent. We also show that the one-dimensional game of life[25] is weakly turbulent. Section 9 is a summary.

2. CHEMICAL TURBULENCE

Kuramoto,[27] Koppel,[28] and other researchers have been conducting extensive and systematic studies of coupled (stable) limit cycles for more than 10 years. One of the most important outcomes is the concept of chemical turbulence.[29],[3]

Usually, we start from an ordinary differential equation which has a unique globally stable limit cycle:

$$\frac{d}{dt}\psi(t) = f(\psi(t)) \tag{2.1}$$

[3] This should not be confused with so-called chemical chaos, which does not include spatial randomness at all.

where ψ is a vector-valued function of time, and f defines a flow field. Without any loss of generality, we may assume that ψ is a 2-vector. We suppose that at each point there is a nonlinear oscillator described by (2.1), and that they are diffusively coupled as

$$\frac{\partial}{\partial t}\psi(r, t) = f(\psi(r, t)) + D\,\Delta\psi(r, t) \tag{2.2}$$

Applying the reductive perturbation method to this equation with the stability argument, Kuramoto derived the following equation, now called the Kuramoto–Sivashinsky equation[27,29,30]:

$$\partial_t\psi + \Delta\psi + \Delta^2\psi - (\nabla\psi)^2 = 0 \tag{2.3}$$

Yamada and Kuramoto[29] showed numerically that the Kuramoto–Sivashinsky equation exhibits turbulent space-time patterns.

Following the Kuramoto–Yamada prediction, Yamazaki *et al.*[31] performed an experimental study of chemical turbulence, using the Belousov–Zhabotinsky reaction.[32] To satisfy the condition for (2.1), they chose the regime of the reaction where there were only purely periodic oscillations when the solution was stirred well; that is, without spatial coupling, the system exhibited only a globally stable limit cycle behavior. Thus, if a chaotic phenomenon was observed in a vessel without any hydrodynamic disturbance, it was solely due to the existence of the spatial inhomogeneity. Actually, eliminating all the hydrodynamic disturbances required extremely careful experiments in contrast to the relatively easy stirred reactor experiments required in the study of chemical chaos. The Belousov–Zhabotinsky reaction is exothermic, and generates carbon dioxide. To prevent any convection due to the exothermicity of the reaction, the reaction vessel (50-ml beaker) had to be cooled slightly from below to eliminate Benard convection (a temperature difference of about 0.5 K was needed). Carbon dioxide bubbles had to be kept on the wall of the vessel by coating it with a fresh natural rubber film for each run and any run with one bubble coming up had to be aborted (hence, the reaction vessel had to be watched carefully throughout each run and the successful runs were less than 50% of all runs). The flow induced by adding reagents at the beginning of each run had to be damped as soon as possible by a damper (experiments in thin layers of solution can avoid hydrodynamic disturbances, but then bubbles can disrupt the single-connectedness of the space).

In the experiments by Yamazaki *et al.* malonic acid was oxidized by bromate ion under the existence of a catalyst, ferroin. The free energy

liberated by the oxidation of malonic acid makes ferroin oscillate between two oxidation states; the color of the reduced state is red, and that of the oxidized state is blue. The oscillation was observed as the electromotive force of a suitably constructed cell. The experimental results are summarized in Fig. 2. Both parameters, α, the ratio of molarities, and Θ, the temperature, control the effectiveness of the diffusion. Specifically, with increasing temperature, the frequency of the reaction increases and the effectiveness of the diffusion decreases. From Fig. 2 we may conclude that there are at least two phases, ordered and not ordered. In the former phase well-defined patterns like scrolls were observed in the reaction vessel, but in the latter phase, only nebulous patterns could be seen. The transition

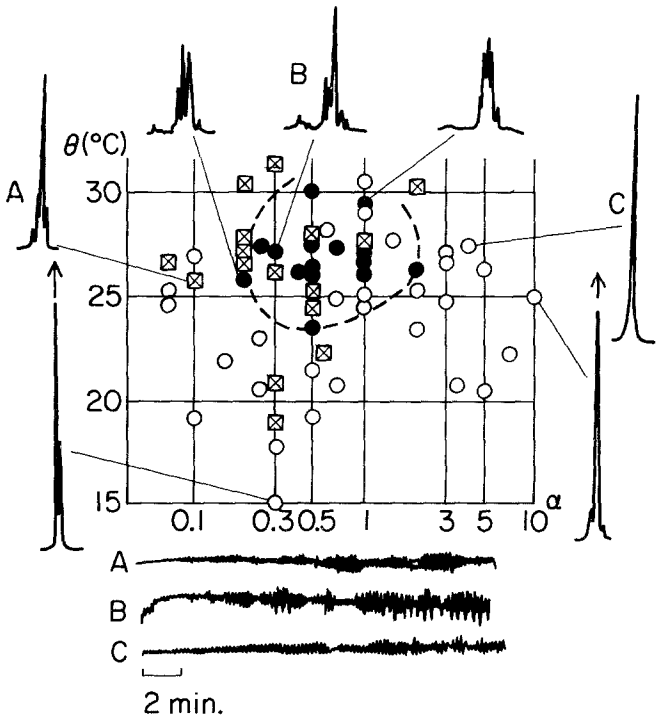

Fig. 2. The phase diagram of a chemical turbulence system.[31] θ is the solution temperature and α is the ratio of molarities, $\alpha = [KBrO_3]/[\text{malonic acid}]$. (●) Disordered; (○) ordered; (⊠) intermediate states according to the order parameter introduced in Ref. 31. The three curves below the diagram are samples of actual emf signals of the cell for *A*, *B*, and *C* points. Other figures describe the voltage spectra of representative points on the phase diagram. There are sharply peaked spectra away from the region circled by a dashed curve. Inside the region the peaks are relatively broad. Although the transition between ordered and disordered seems continuous, there is a fairly well-defined region of the disordered phase.

between these two phases seemed to be continuous. For more details refer to the original report.[31] The observed results are in rough conformity to the following general theoretical results: (1) If the diffusion constant is too small or too large, there is no chemical turbulence; (2) if the degree of the spatial inhomogeneity is too large, then amplitude turbulence occurs[33]; i.e., random modulation of the envelope curve of the signal appears; (3) finite-dimensional caricatures of (2.2)[33] exhibit chaotic phases characterized by temporal alternation of oscillatory behavior and transient disorder behavior (intermittency).

3. CDS MODELS OF CHEMICAL TURBULENCE

3.1. Construction of Models

We construct our model of chemical turbulence in two steps. First, we construct a dynamical model of a single isolated cell. We suppose that the dynamics of the cell is identical to that of the completely stirred isolated system. Next, we couple these cells via linear diffusion.

As is discussed in the preceding section, the essence of chemical turbulence is the linear coupling of orbitally stable limit cycles. Hence the single cell dynamics must be the one with a globally stable limit cycle. The easiest way to mimic this is to use cyclically arranged discrete concentration levels. The state of an isolated cell itinerate these states periodically. Thus, in general, the single-cell discrete dynamics can be expressed as

$$\psi(n, t+1) = F(\psi(n, t)) \tag{3.1}$$

where $\psi(n, t)$ is the concentration in the nth cell at time t, and the map F is a cyclic permutation (i.e., an ergodic automorphism) of a finite set A of discrete concentration levels. The linear coupling is mimicked by the following local weighted average (in 1-space):

$$\psi(n, t+1) = (1-\alpha)\,\psi(n, t) + \alpha[\psi(n-1, t) + \psi(n+1, t)]/2 \tag{3.2}$$

where $\alpha \in [0, 1]$ may be regarded as the diffusion constant. Thus, the overall dynamics of our cell model is given by

$$\psi'(n, t) = (1-\alpha)\,\psi(n, t) + \alpha[\psi(n-1, t) + \psi(n+1, t)]/2 \tag{3.3}$$

and

$$\psi(n, t+1) = F(\{\psi'(n, t)\}) \tag{3.4}$$

where $\{*\}$ denotes some prescription to assign an element in A to $*$.

Roughly speaking, the dynamics describes the repeated readjustments of the internal clock of each cell to the averaged time of its neighborhood cells.

The simplest choice of A would be a two-symbol set. We can choose 0 and M for the two concentration levels without any loss of generality, where M is a number greater than 0.5. Now F is given by

$$F(0) = M, \qquad F(M) = 0 \tag{3.5}$$

and the $\{\ \}$ is defined as

$$\{x\} = \begin{cases} M & \text{if } 0.5 \geqslant x \\ 0 & \text{if } x > 0.5 \end{cases} \tag{3.6}$$

Depending on the values α and M, the model becomes identical to various two-state CA (01-CA), as is summarized in the phase diagram (Fig. 3). None of these CA gives nontrivial stationary patterns.

The next simplest choice for the set A is the three-symbol set. For

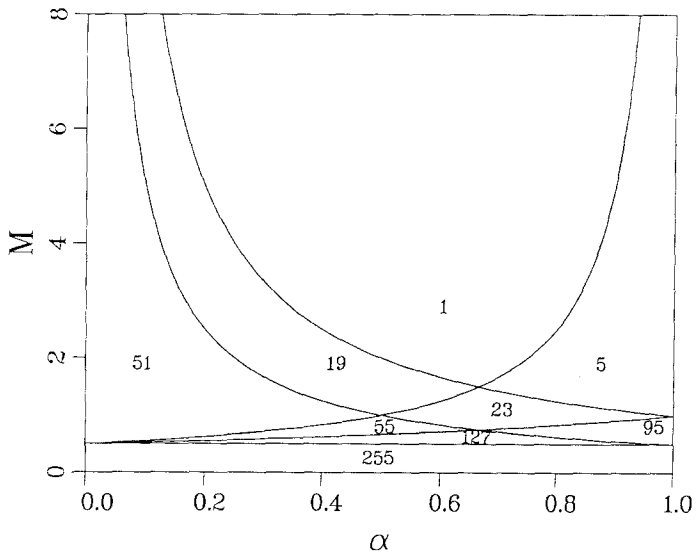

Fig. 3. The phase diagram for the $0M$ model with the corresponding 01-CA rule numbers.[1] Here α is the diffusive coupling strength and M is the peak value of the autonomous oscillation.

simplicity, A is chosen as $\{0, 1, M\}$, where M is a number larger than 1.5. Now F and $\{\ \}$ are defined as follows:

$$F(\{x\}) = \begin{cases} 1 & \text{if } 1.5 \leqslant x \\ 0 & \text{if } 0.5 \leqslant x < 1.5 \\ M & \text{if } x < 0.5 \end{cases} \tag{3.7}$$

The nicety of the present model was stressed by Kohmoto[4] in the early stage of the present study. As we will see soon, the model can exhibit non-trivial phases, in contrast to the two-state model. We have also studied an analogous model with $A = \{0, 1, 2, M\}$, where M is a number greater than 2.5, and have found richer dynamical behavior. However, the three-level model is sufficiently rich for the purpose of the present paper, so henceforth we concentrate on this model, which we call the $0M1$ model.

3.2. Experimental Results on the $0M1$ Model

The phase diagram for the $0M1$ model is shown in Fig. 4. Typical space-time patterns, autocorrelation functions for the single cell states,

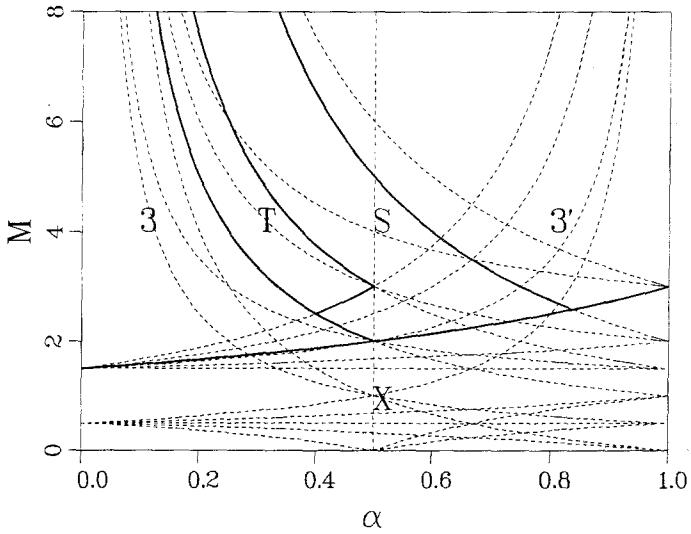

Fig. 4. The phase diagram for the $0M1$ model. The dashed lines are boundaries of areas with the same local rules. The solid line indicate different macroscopic phases. The symbols 3 and 3′ are the two periodic phases with period three, and T and S are the T-phase and the S-phase. As in the real experiment, there is a turbulent (T) region at intermediate values of diffusion sandwiched between two ordered regions (3 and 3′). The letter X denotes other phases not discussed in the text.

corresponding power spectra, and spatial correlation functions are shown in Fig. 5. Although we specified our dynamics with Eqs. (3.3) and (3.4), we could have done the same job by tabulating all the local rules, i.e., the map $f: A^3 \to A$ such that

$$f(\psi(n+1, t), \psi(n, t), \psi(n-1, t)) = \psi(n, t+1)$$

as in the ordinary CA. The dotted curves in the phase diagram (Fig. 4) denote boundaries for different local rules. We immediatedly realize from this phase diagram that different local rules, say, the three sectors in the T-phase, can give the same phase (at least apparently). As we will see soon, the S-phase is subdivided into S_a and S_b, and within each of the T, S_a, and S_b phases, effective local rules are identical. By *effective local rules* we mean the local rules actually used in the "stationary" space-time patterns. By the word "stationary" we mean the periodic state of a CA on a finite lattice. The word will be carefully defined for the case of infinite lattices in the next section. Table I shows the local rules and the effective local rules for the T- and S-phases. Notice that many different local rules give an identical effective rule. These empirical results will be proved in Section 6.

The periodic phases 3 and 3′ are not characterized by unique effective rules, but since these phases are not interesting, we will not discuss them further. Inspection of Table I shows that the difference between the S-phase

3 T S 3′

Fig. 5a. Typical space-time patterns of the $0M1$ model.[4] Time flows from top to bottom. The horizontal direction is the spatial direction. The empty cells actually contain M. The T-phase exhibits weakly turbulent space-time patterns. In the infinite-system limit the S-phase would look homogeneous to any local observer. 3 and 3′ are the two period-three phases.

and T-phase consists of the presence of the two effective local rules for the triplets 101 and $M0M$. The S-phase lacks all these rules because isolated zeros never appear and these local configurations are forbidden. This is because, even if such local patterns exist in the initial configurations, they disappear due to the efficiency of the diffusive coupling in the S-phase. In contrast, the T-phase does not have such an efficient diffusion, so that spatial homogeneity does not appear. As we see in Fig. 5c, the time correlation function in the T-phase exhibits a kind of long-time tail which decays algebraically. This is not surprising, since the $0M1$ model and

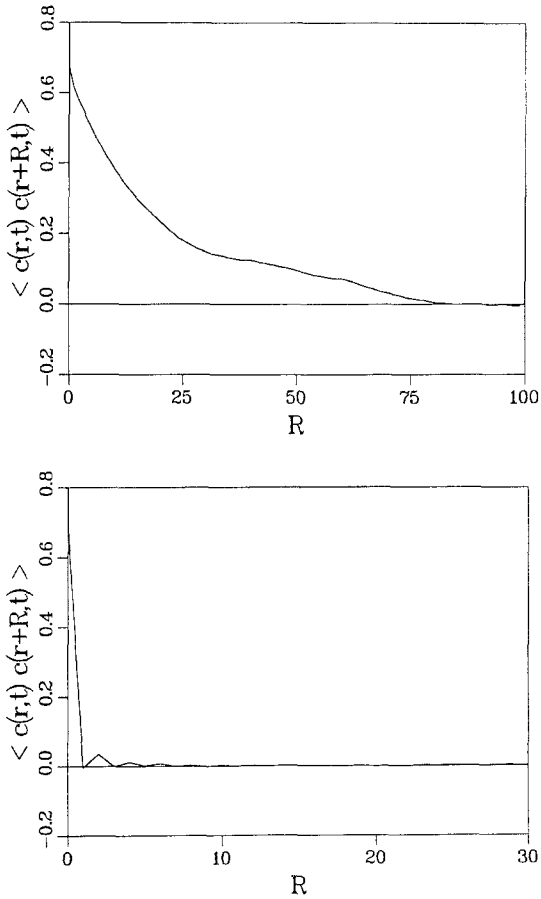

Fig. 5b. The space correlation functions $\langle c(r, t)\, c(r+R, t)\rangle_{r,t}$ obtained from simulations on a 400-site lattice. In the T-phase (bottom) the correlation decays to zero (within statistical error) in fewer than ten sites. In the S-phase the decay is much slower.

Niwa's hard rod system,[34] for which the correlation function decays as $t^{-1/2}$, are similar, as we will see in Section 6.

Our powerful visual pattern recognition ability tells us that the phase T is different from other phases; although we recognize some regularity, it looks rather random. We would say that the phase is (at least weakly) turbulent. Thus, we call the phase T (turbulent). We postpone, to Section 8, however, answering the question of whether the phase T may be reasonably called turbulent. In a preliminary report of this study by Oono

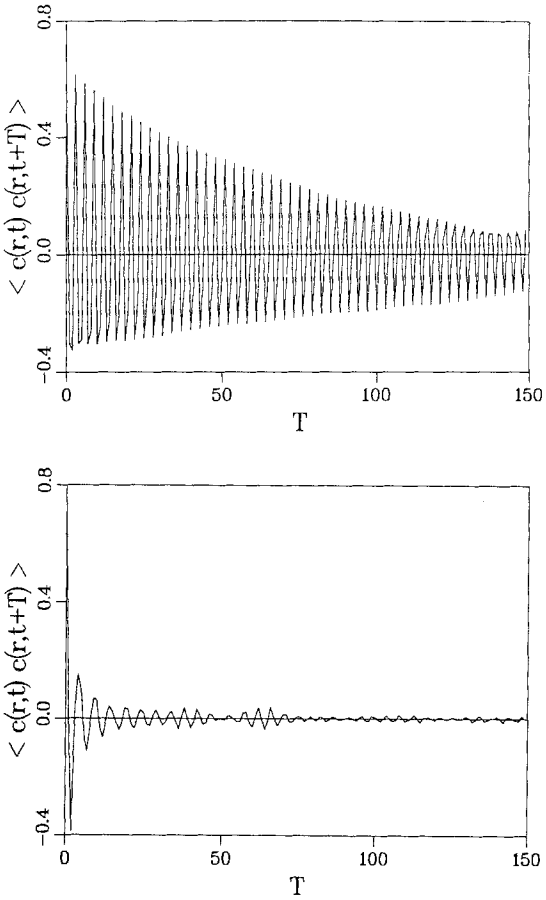

Fig. 5c. The time correlation functions $\langle c(r, t)\, c(r, t+T)\rangle_{r,t}$ obtained from simulations on a 250-site lattice. In the S-phase (top) the initial decay is exponential, but the decay time is long. In the T-phase (bottom) there is a much more rapid initial decay, followed by a long-time tail. The small cycles reflect the periodicity of the single-cell dynamics.

and Kohmoto,[4] phases were tentatively characterized by the values of the Markov entropies[35] of the spatial and temporal structures. These entropies give upper bounds to the sequence entropies, whose definition can be found in Section 7. However, in order to calculate, e.g., the Kolmogorov–Sinai entropy of a CA, we must use an infinitely large lattice. Otherwise, any state of the system obtained in the large-time limit must be periodic, so that any dynamical entropy trivially vanishes. In any case, since the most important part of the theory of dynamical systems is the

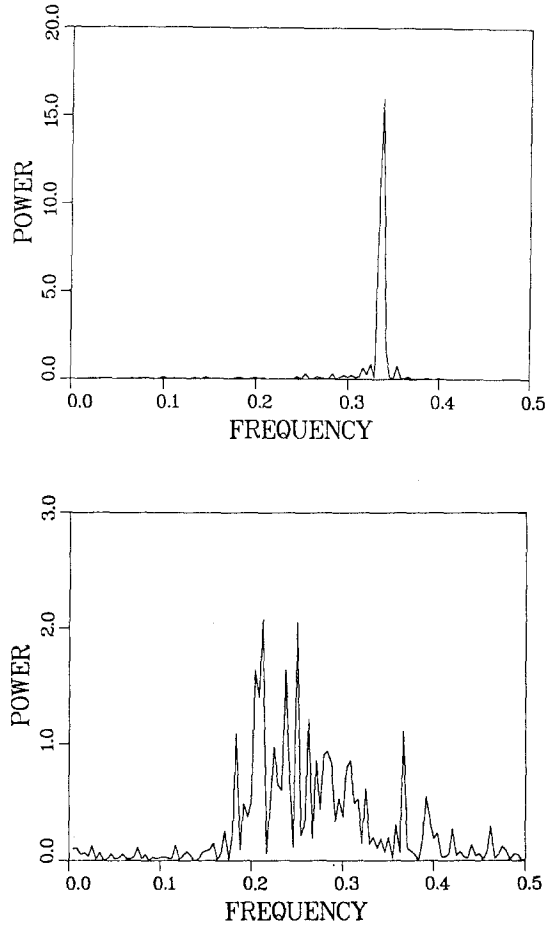

Fig. 5d. The power spectra for the T- and S-phases. The power spectrum of the T-phase is broad and has maxima at $f = 0.2$ (period 5) and $f = 0.25$ (period 4). These frequencies are present during collisions. In the S-phase the power spectrum is sharp, with a peak at $f = 0.33$ (period 3).

Table I. Local Rules for Subphases in the *T* and *S* Phases[a]

Sub-phases	Triplets																			
	00*M*	001	00*M*	101	10*M*	*M*0*M*	010	011	01*M*	111	11*M*	*M*1*M*	0*M*0	0*M*1	0*MM*	1*M*1	1*MM*	*MMM*	*M*	α
T_1	**M**	**M**	**0**	**M**	**0**	**0**	**0**	**0**	0	**0**	0	1	**1**	1	**1**	1	1	**1**	4	0.3
T_2	**M**	**M**	**0**	**M**	**0**	**0**	**0**	**0**	0	**0**	1	1	**1**	1	**1**	1	1	**1**	6.5	0.2
T_3	**M**	**M**	**0**	**M**	**0**	**0**	**0**	**0**	1	**0**	1	1	**1**	1	**1**	1	1	**1**	7.25	0.2
S_{a1}	**M**	**M**	**0**	*M*	**0**	1	**0**	**0**	0	**0**	1	1	**1**	1	**1**	1	1	**1**	4	0.4
S_{a2}	**M**	**M**	**0**	*M*	**0**	1	**0**	**0**	1	**0**	1	1	**1**	1	**1**	1	1	**1**	6	0.4
S_{b1}	**M**	**M**	**0**	*M*	**0**	0	0	**0**	0	**0**	0	1	0	1	**1**	1	1	**1**	2.75	0.49
S_{b2}	**M**	**M**	**0**	*M*	**0**	0	0	**0**	0	**0**	0	1	0	0	**1**	1	1	**1**	2.25	0.49
S_{b3}	**M**	**M**	**0**	0	**0**	0	*M*	**0**	0	**0**	0	1	0	1	**1**	1	1	**1**	2.75	0.51
S_{b4}	**M**	**M**	**0**	0	**0**	0	*M*	**0**	0	**0**	0	1	0	0	**1**	1	1	**1**	2.25	0.51
S_{b5}	**M**	**M**	**0**	0	**0**	0	*M*	**0**	0	**0**	0	1	0	0	**1**	0	1	**1**	2.25	0.625
S_{b6}	**M**	**M**	**0**	0	**0**	1	*M*	**0**	0	**0**	0	1	0	0	**1**	1	1	**1**	2.77	0.55
S_{b7}	**M**	**M**	**0**	0	**0**	1	*M*	**0**	0	**0**	0	1	0	0	**1**	1	1	**1**	2.50	0.62
S_{b8}	**M**	**M**	**0**	0	**0**	1	*M*	**0**	0	**0**	0	1	0	0	**1**	0	1	**1**	2.38	0.675
S_{b9}	**M**	**M**	**0**	0	**0**	1	*M*	**0**	0	**0**	1	1	1	1	**1**	1	1	**1**	3.50	0.525
S_{b10}	**M**	**M**	**0**	0	**0**	1	*M*	**0**	0	**0**	1	1	0	1	**1**	1	1	**1**	3	0.525
S_{b11}	**M**	**M**	**0**	0	**0**	1	*M*	**0**	0	**0**	1	1	0	0	**1**	1	1	**1**	3	0.65
S_{b12}	**M**	**M**	**0**	0	**0**	1	*M*	**0**	0	**0**	1	1	0	0	**1**	0	1	**1**	2.55	0.7
S_{b13}	**M**	**M**	**0**	0	**0**	1	*M*	**0**	1	**0**	1	1	1	1	**1**	1	1	**1**	4	0.575
S_{b14}	**M**	**M**	**0**	0	**0**	1	*M*	**0**	1	**0**	1	1	0	1	**1**	1	1	**1**	3.75	0.62

[a] Only 18 triplets are shown, since the rules for the other triplets can be obtained by symmetry. The effective local rules (those present in the stationary state) are shown in boldface. A region is in the *T*-phase if both $M0M \to 0$ *and* $0M0 \to 1$. A region is in phase S_a if both $010 \to 0$ *and* $0M0 \to 1$. A representative point of each subphase is listed.

study of long-time behavior of dynamical systems, we must study CA on infinite lattices. Then we must be careful when we define the stationary states of CA, because transient behavior could be infinitely long on infinite lattices. Indeed, our phases S and T exhibit such behavior. We will see in Section 6 that the true stationary state in the S regime does not contain any soliton-like elementary excitations. The S phase reminds us of the excitable state of the Belousov–Zhabotinsky system.[36,37] These subtleties were not discussed in our preliminary report. The existence of extremely long transient behavior has been noted in ordinary CA.[38] We will discuss how to define the large-size limit of CA in the next section. After making this limit meaningful, we consider this limit in the T- and S-phases.

4. STATIONARY STATE OF CA

In the study of ordinary dynamical systems we pay attention primarily to their stationary states, or the behavior on their ω-limit sets. For example, to calculate the Liapunov characteristic number (LCN) unambiguously, we require that the system is in an ω-limit set. We must note that no CA system so far studied numerically has ever been in a nontrivial stationary state (here, "nontrivial" means "not periodic"); on computers we can study only finite-size lattice systems, so that true stationary states are merely periodic states. If one wants to study a CA from the computation-theory point of view or to use CA as, for example, an encoder, it may be rather silly to study its long-time statistics. Here, however, we study CA as models of nonequilibrium statistical physics, so that we must first clarify what is meant by the long-time behavior.

In this section, we define empirically accessible invariant states of CA on infinite lattices in a rather abstract setting. Then, we study the invariant states of the $0M1$ model, showing the uniqueness of the "turbulent" phase in Sections 5 and 6.

4.1. Empirical and Observable Measures

We consider, for simplicity, the 1D nearest neighbor models with the finite cell state A. That is, we consider a CA, $T: A^Z \to A^Z$ defined as

$$T\{a_i\}_{i=-\infty}^{+\infty} = \{a_i'\}_{i=-\infty}^{+\infty} \tag{4.1}$$

with

$$a_i' = f(a_{i-1}, a_i, a_{i-1}), \qquad \text{for} \quad i \in Z \tag{4.2}$$

where $f: A^3 \to A$ is a map defining the local rules of CA. For general CDS

we must study all the periodic orbits of finite lattice systems, and can proceed similarly for CA. An explicit construction will be postponed for future publication. In this subsection we outline how to construct T-invariant measure on A^Z to define measure-theoretic CA. A mathematical account can be found in the Appendix. We summarize the discussions and results of the Appendix in the remaining part of this subsection.

The main motivation behind our construction is as follows. In the case of axiom A dynamical systems[39] and endomorphisms of intervals,[40] the statistical behavior is completely determined by the periodic orbits. This situation is quite parallel to that of ordinary statistical mechanics.[5] We can take the thermodynamic limit starting from finite systems with periodic boundary conditions. In the case of CA we proceed analogously. We take a CA on a finite lattice with periodic boundary condition and study all the periodic states. Then we take the infinite-lattice-size limit. We show that this limit is well-defined. It may seem natural that if the system is sufficiently "turbulent," then the limit is unique. We will see this is the case for our T-phase of the $0M1$ model.

We begin by taking the statistics of local configurations (finite-length words) around a fixed cell denoted by O, where we suppose that the observer is located. The observer cannot see far away nor remember far back accurately. Since we can simulate or observe only finite lattice for finite time spans, we are much like this observer.

We proceed as follows. Take a both-side infinite sequence $\mathbf{a} \in A^Z$ as an initial condition, for which we want to define the stationary states. Then, cut out from $\mathbf{a}$ the finite subsequence of length N, $\mathbf{a}_N$, centered around the observer O and make a ring by pasting together the ends of the cutout finite sequence. Next, obtain the periodic orbit of this finite periodic lattice system with the initial configuration $\mathbf{a}_N$ under the same local rules designated by f. We take the statistics of the appearance of all the local configurations around the observer (i.e., the spatial patterns occupying connected subsets of the lattice centered around the observer; see Definition 5 in the Appendix for a more precise description). Thus, we make a statistical table of local patterns, which can be regarded as a vector. For each N we can make such tables (vectors). For each infinite sequence $\mathbf{a}$ in A^Z we can make the set of all such tables [which is the set $P_{\mathbf{a}}$ in (A.11) of the Appendix] and look for its accumulation points with respect to the metric that is in conformity with the limitations of our observer at O. Each accumulation point is again a statistical table of local configurations. The obtained probabilities for local configurations satisfy the Kolmogorov extension theorem.[41] Hence, for each accumulation point we can define a T-invariant measure on A^Z, which we call an *empirical measure*. Any empirical measure is ergodic (but not necessarily mixing). We identify

invariant measures and stationary states. As can be guessed from the above argument, even with only one **a**, we need not have a unique invariant measure. However, different initial vectors **a** may give the same invariant measure. If we can get an empirical measure μ from "many" initial vectors $\mathbf{a} \in A^Z$, we say that μ is *observable* (see, more precisely, Definition 7 in the Appendix).

An observable invariant measure μ constructed as above is experimentally accessible at least in principle. The triplet (T, μ, A^Z) defines a measure-theoretic CA. The most important feature of a T-invariant measure we constructed is that it is completely determined by spatially localized cylinder sets around the observer. There can be many other invariant measures, which cannot be specified by these local cylinder sets. Although these measures are perfectly admissible in the definition of measure-theoretic dynamical systems, we will not consider these pathological measures.

4.2. Elementary Examples

There are cases without any observable invariant measures (as defined in the previous section). The most obvious case is for T being the identity map on A^Z.

Almost trivial but nonetheless useful examples (as counterexamples) follow.

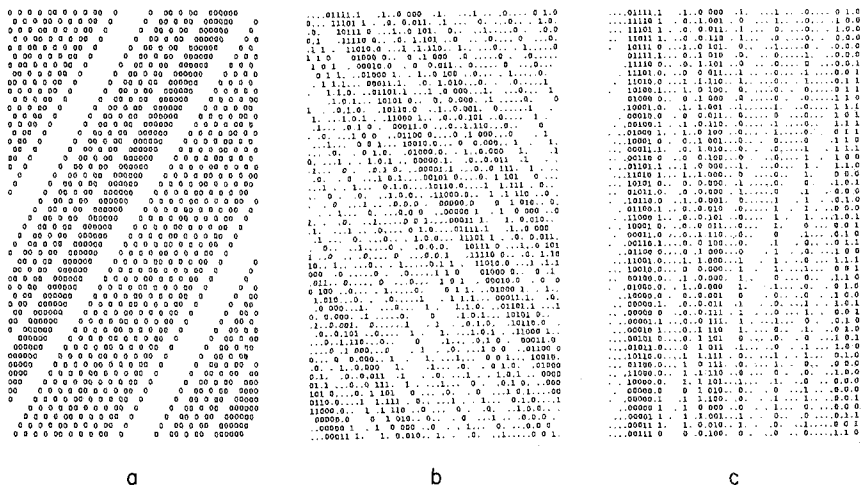

a b c

Fig. 6. Typical space-time patterns for the counterexamples discussed in Section 4.2. (a) Single direction shift, (b) double direction shift, (c) single direction shift imposed on a "frozen" background.

Example A. If $T: A^Z \to A^Z$ is defined by the local rules such that

$$f(a, b, c) = c, \qquad a, b, c \in A \tag{4.3}$$

then (T, A^Z) is called a *shift* dynamical system. This system has the unique observable invariant measure given by ν in Definition 7 of the Appendix. The measure-theoretic dynamical system (T, ν, A^Z) is isomorphic to the Bernoulli automorphism $B(p,..., p)$,[26] where $p = 1/\#(A)$, so this is a chaotic dynamical system with the Kolmogorov–Sinai entropy $\log \#(A)$. A typical space-time pattern is shown in Fig. 6a.

In this example on a lattice of size N, the periodic orbit contains at most N points in A^N, so that it is a very tiny subset of A^N for large N. Notice that still the invariant measure constructed from this orbit is ergodic on A^Z.

Example B (Double shift). Consider the 1D, four-state $\{0, 1, 2, 3\}$ nearest neighbor CA whose local rule f is solely determined by the first and the third coordinates as

$$f(a, b, c) = g(a, c) \tag{4.4}$$

where g is given by Table II. In this case the observable invariant measure is again unique and given by ν. The resultant system $(T, \nu, \{0, 1, 2, 3\}^Z)$ is isomorphic to the direct product of two $B(1/2, 1/2)$ systems, so that[42] it is isomorphic to $B(1/4, 1/4, 1/4, 1/4)$. The present example is called a double shift; the cell state is specified by a two-bit number and f is a left shift on the lower bit and a right shift for the higher bit. Hence the system is the direct product of two shifts on two symbols. A typical space-time pattern for the this model is shown in Fig. 6b.

Table II. Table for Function $g(x, y)$ Used in Examples A and B[a]

		y			
		0	1	2	3
x	0	0	1	0	1
	1	0	1	0	1
	2	2	3	2	3
	3	2	3	2	3

[a] The function can be written $g(x, y) = x - (x \bmod 2) + (y \bmod 2)$.

Example B corresponds to the 1D, infinite ideal gas system, which is known to be Bernoulli. The reasons this system[43] is Bernoulli and example B is Bernoulli are parallel: local disturbances "fly off" unhindered to infinity, where they are no longer observable, never to return.

The double-shift construction is an easy way to make a chaotic reversible CA.

These examples clearly show that whether a system is Bernoulli [or Kolmogorov (K)[26]] has *no* direct relation to the "complexity" of the space-time patterns.

Example C. Consider the 1D, four-state $\{0, 1, 2, 3\}$ nearest neighbor CA whose local rule f is determined by the second and the third coordinates as

$$f(a, b, c) = g(b, c) \tag{4.5}$$

where g is the same as in example B. Here f is a left shift for the lower bit and the identity map for the higher. In this case there is no observable invariant measure. The reason is exactly the same as in the identity map case. However, this example has many invariant measures that make the system isomorphic to $B(1/2, 1/2)$. A typical space-time pattern is shown in Fig. 6c.

5. STATIONARY STATE OF 0*M*1 MODEL

In Section 3 we have empirically given various phases. Periodic phases are obviously nonturbulent, although spatial randomness due to initial randomness may be preserved. We have observed three nontrivial phases T, S_a, and S_b. In this and the next sections we consider stationary states on infinite lattices. We will see in the next section that there are only two distinguishable phases in the parameter range of these three phases on infinite lattices.

As in many problems of statistical mechanics, we are interested in the question of whether we can predict macroscopic phases from microscopic dynamics (in our case from local rules f). Fortunately, in our $0M1$ model we can accomplish this goal rigorously. This will be demonstrated in this and the following section. Our strategy can be summarized as follows:

1. We begin with the $0M1$ system with uniform product measure μ_0 on $\Omega_0 \equiv \{0, 1, M\}^Z$ as the initial measure. This system is denoted by (T, Ω_0, μ_0). Notice that here, (T, Ω_0, μ_0) does not imply a measure-theoretic dynamical system, since μ_0 is not necessarily invariant. This is also true for the systems in items 2 and 3.

2. We show that there are no adjacent M and 1 after two updates. The system obtained from (T, Ω_0, μ_0) after two updates will be denoted by (T, Ω_1, μ_1) (Section 5.1).
3. We define a one-to-one map $\phi: (T, \Omega_1, \mu_1) \to (T', \Omega_2, \mu')$, which takes the system to a kind of 1D hard-rod dynamical system (the P-I system as defined in Sections 5.2 and 5.3). This system will be used to find the effective local rules for the T- and S-phases.
4. We define another one-to-one map $\theta: (T', \Omega_2, \mu') \to (S, \Omega_3, \nu)$, which takes the system to an "almost" independent two-color-particle system, P-II. We will use this system to find the observable invariant measure ν_∞ and demonstrate that the measure defines a Gibbs random field (Section 6). Thus, the statistics of the spatial pattern can be obtained, in principle, from a partition function. Furthermore, we will use this map to show that the T-phase is "weakly" turbulent (Sections 7 and 8).

Thus, starting from the local rules, we can completely predict the macroscopic states of the two phases.

5.1. Absence of Adjacent M and 1

The S- and T-phases are differentiated by the local rule for the triplets $M0M$ and $0M0$. If both $M0M \to 0$ and $0M0 \to 1$, then the system is in the T-phase. Furthermore, the S-phase can be divided into two phases, labeled S_a and S_b. In the S_a-phase $010 \to 0$ and $0M0 \to 1$. These rules have a small probability of presence on finite lattices in the stationary state of phase S_a. We will see that the difference between S_a and S_b is observable only for finite systems.

Before proceeding with the analysis we introduce some standing notation.

$\#$ indicates "wild card," meaning any cell state is allowed.

$\check{x}$ indicates "not state x," meaning any cell state is allowed except x.

$*x$ (resp. $x*$) denotes the sequence $...xxx$ (resp. $xxx...$).

(abc) denotes the triplet abc.

$[a...z]$ denotes the totality (cylinder sets) of configurations containing the local configuration $a...z$ around the observer.

We claim: Starting from any initial configuration in the T- and S-phases, there is no spatial configuration containing M adjacent to 1 after two time steps. (Hence, any stationary spatial pattern cannot contain local configurations $M1$ and $1M$.)

Proof. Let M^0 and 1^0 be the following subsets of A^3:

$$\begin{aligned} M^0 &= \{(abc): f(a, b, c) = M\} \\ 1^0 &= \{(abc): f(a, b, c) = 1\} \end{aligned} \tag{5.1}$$

Of course, these depend on f, which is different from subphase to subphase. From inspection of Table I we see that $M^0 \subset \{(\check{M}0\check{M}), (010)\}$ for all subphases in the T- and S-phases. In order for local configuration $1M$ to exist at time $t+1$, $T^{-1}([1M])$ must not be empty. Therefore, if $1M$ exists, then there must be triplets $(\#\check{M}0)$ or $(\#01)$ at time t such that $f(\#, \check{M}, 0)$ or $f(\#, 0, 1) = 1$. From inspection of Table I in subphases T_1, T_2, S_{a1}, and S_{b1} through S_{b12}, we have

$$1^0 \subset \{(\#M\#), (\check{0}1\check{0}), (M0M)\} \tag{5.2}$$

implying

$$1^0 \cap \{(\#\check{M}0), (\#01)\} = 0 \tag{5.3}$$

Thus, there is no $1M$ after the first update in these subphases. By symmetry, $M1$ is also not allowed. In the remaining subphases, T_3, S_{a2}, S_{a3}, S_{b13}, and S_{b14}, the situation is a little more involved. From Table I we have

$$1^0 \subset \{(\#M\#), (\check{0}1\check{0}), (M10), (01M), (M0M)\} \tag{5.4}$$

Therefore

$$\begin{aligned} 1^0 \cap \{(\#\check{M}0), (\#01)\} &= (M10) \\ 1^0 \cap \{(0\check{M}\#), (10\#)\} &= (01M) \end{aligned} \tag{5.5}$$

However, in these subphases $f(\#, M, 1) = 1$, so that $T([M10])$ cannot be in $[01M]$ or $[M10]$. By symmetry, $T([01M])$ cannot be in $[M10]$ or $[01M]$. Therefore, there are no local configurations of the form $01M$ or $M10$ at time $t+1$ and thus no configurations containing $M1$ or $1M$ at time $t+2$. ∎

Thus, all the local rules containing $1M$ and $M1$ are disqualified as effective local rules. We must show which of the remaining local rules survive as effective rules. To this end, we map our system to an interacting particle system.

5.2. Mapping to Particle System I

We now show that the system without any M adjacent to 1 can be considered to be a system of interacting solitons. Toward this end we introduce a consistent definition of the soliton direction and position.

Any inhomogeneity must be with the local configuration $X0Y$, where X and Y are not simultaneously 0, since M and 1 cannot be adjacent. We define the positions and the directions of propagation of solitons as in Table III. Figure 7 illustrates some of these solitons.

A pair of left-going and right-going solitons can only be in collision configuration if they are within two lattice sites. Actually, collision configurations must contain one of the following local configurations: $M00M$, $M0M$, 1001, or 101 (see Fig. 7). Local configurations $M00M$ and $M0M$ are just before the collision and 1001 and 101 are just after.

If a soliton is not associated with any collision configuration, then it stays at the same interstice for three time steps. We can introduce a phase variable $\varphi \in \{0, 1, 2\}$ to specify how long the soliton has been at the same interstice. If $\varphi = 2$ and no collision occurs, the soliton moves to the nearest neighbor interstice according to its direction and φ becomes 0. Collisions occur only between $\varphi = 2$ solitons. Immediately after the collision the phase variables of solitons involved in the collision becomes 1. The phase variable otherwise increases by unity at each time step. If we specify the position, the direction, and the phase of each soliton, then we can uniquely map the original spatial configuration to a system of solitons with internal phases.

Now we eliminate the phase variable φ by mapping to a system in which the particle moves one site per step. For a lattice of size N, we prepare another lattice of size $3N$ both with periodic boundary conditions. The phase, position, and direction of a soliton on the original N lattice is mapped into a left- or right-going particle on the $3N$ lattice as follows. A right-going (left-going) soliton between the n and $n+1$ cells with phase φ

Table III. Direction and Phases of a Soliton between Sites n and $n+1$ in the $\{0, 1, M\}$ Representation and the Corresponding Position in the P-I Representation[a]

Configuration	Phase	Direction	Position in P-I
$\#1\underline{0}M\#$	0	Right	$3n$
$\#\breve{M}\underline{0}1\#$	1	Right	$3n+1$
$\#\underline{M}0\breve{1}\#$	2	Right	$3n+2$
$\#\underline{M}01\#$	0	Left	$3n+2$
$\#\underline{1}0\breve{M}\#$	1	Left	$3n+1$
$\#\breve{1}\underline{0}M\#$	2	Left	$3n$

[a] Site n is marked by

is mapped into a particle at the $3n+\varphi$ $(3n+2-\varphi)$ cell in the new $3N$ lattice. Thus, via the intermediate soliton picture we can injectively map any spatial configuration allowed in the stationary state of T- and S-phases to a many-particle system. Let us denote this map ϕ, and call the system the P-I system.

The configuration of particles in the P-I system has several restrictions. The most important one is that two neighboring particles traveling in the same direction must be separated by $5+3i$ $(i=0, 1, 2,...)$ lattice spacings. The minimum separation between two particles on the N lattice is given by $10\,\|M\|\,0\check{1}$ ($\|$ indicates the location of the soliton), which is separated by five lattice spacings on the $3N$ lattice. Since all neighboring particles traveling in the same direction must have the form $10\,\|M...M\|\,0\check{1}$ for one of the phases and the separation on the $3N$ lattice is independent of phase, the distance on the $3N$ lattice must be $5+3i$ $(i=0, 1, 2,...)$ lattice spacings. Other restrictions can be obtained in the same manner: two neighboring particles traveling in the opposite direction are separated by $3+3i$ $(i=0, 1, 2,...)$ lattice spacings if they are traveling away from one another and $1+3i$ $(i=0, 1, 2,...)$ lattice spacings if they are traveling toward each other (see Fig. 7). The subset of all the particle configurations on the $3N$ lattice with these constraints is invariant, if the dynamics is specified through the original $0M1$ dynamics. This dynamics, $\phi T\phi^{-1}$, will be detailed in terms of particles in the next subsection. This map ϕ is one-to-one between the original configuration without adjacent M and 1 and the particle configuration on the $3N$ lattice with these constraints.

5.3. Collisions of Particles in the P-I System

We claim that the interactions among particles on the $3N$ lattice are all binary interactions.

To discuss collisions it is convenient to introduce the parity of a particle. We define the parity of a particle as even if it occupies an even-numbered site at an even time step from an arbitrarity chosen $t=0$ and an odd-numbered site at an odd time step. Otherwise, the particle has odd parity. (The parity is defined only locally around O, since we use periodic lattices.)

There are two types of collisions in the P-I representation in the phase T and the phase S_a. If the colliding particles have the same parity (separated by an even number of lattice spacings), then the collision occurs after the particles become four lattice spacings apart and both particles change directions after the collision (Fig. 7a). If the colliding particles have different parities, they do not interact until after they are adjacent to each other. In the S_a-phase the particles then annihilate each other (Fig. 7b). In the T-phase they merely change directions (Fig. 7c). It should be noted that

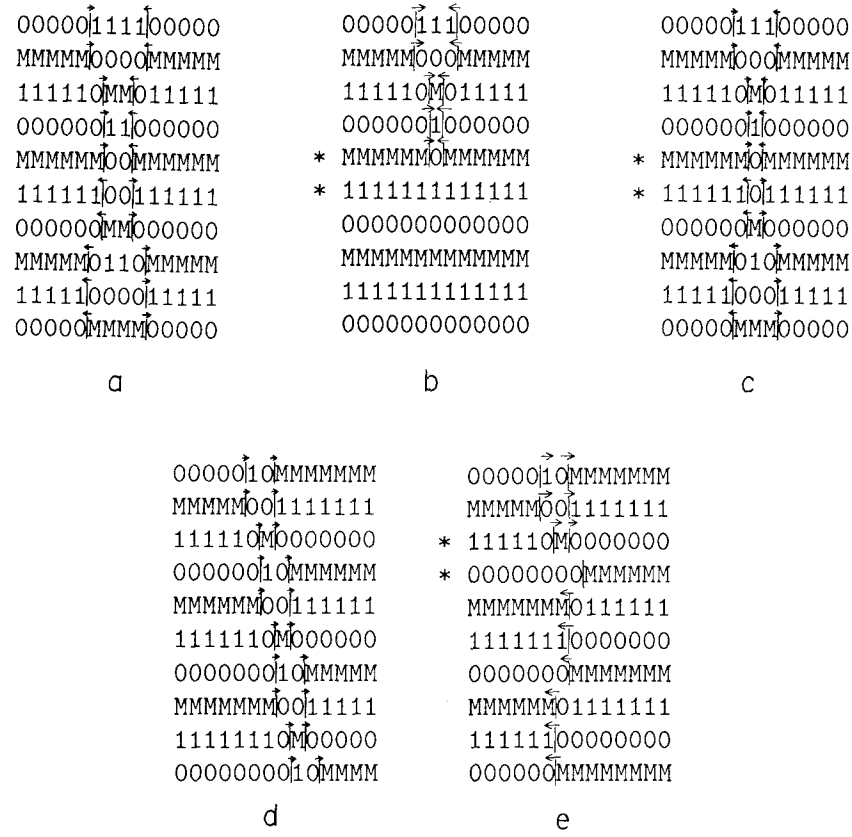

Fig. 7. (a) A same-parity collision (same in both S- and T-phases). The soliton positions are marked by a line and the arrow indicate the direction of propagation. The time steps marked by asterisks are the collision configurations. (b) An opposite-parity collision in the S-phase. The solitons are annihilated in the collision. (c) An opposite-parity collision in the T-phase. The solitons survive the collision. (d) A double wall (two solitons traveling in the same direction separated by the minimum distance) propagating in the T- and S_a-phases. (e) A collision in a double wall in the S_b-phase.

in both cases the parity of the colliding particles is conserved when the particles survive.

In phase S_b, in addition to the two types of collisions mentioned above, there is an additional interaction, which occurs when two solitons traveling in the same direction are separated by five lattice spacings (the minimum separation between the two particles) (Fig. 7d). In this case the trailing soliton is destroyed and the leading soliton changes direction (Fig. 7e).

We must show that all interactions among particles in the P-I system can be accounted for by using the binary interactions considered above. Since the particles are local objects, all two-particle interactions are taken care of by these binary interactions. There can be no longer range binary interaction than those already given. Therefore, we just need to ascertain that there is no interaction involving more than two particles. Consider two neighboring particles traveling in the same direction. The separation must be $5+3i$ ($i=0, 1, 2,...$). Therefore, if the leading particle is involved in a collision, the separation between the two particles will be $3+3i$ ($i=0, 1, 2,...$) immediately after the collision. This separation is wider than the interaction length (1 for odd separation and 4 for even), so that the second particle does not interfere with the first collision.

Thus ϕ maps the original system to a many-particle system with binary interactions. Notice that $\phi^{-1}\phi$ is the identity. The system can be regarded as a slightly complicated hard-rod system.

Finally we mention another possible interpretation of the result of the collisions. Instead of viewing the particles as changing directions upon collision, we can interpret the collision as the two particles passing through each other. In this case, if two particles are involved in a same-parity collision, each particle moves five lattice spacings in the direction of propagation instead of just one. During an opposite-parity collision each particle moves two lattice spacings instead of one. This interpretation has the advantage that same-parity collisions would preserve individual direction as well as parity.

5.4. Effective Rules for Finite Systems

In the S-phase, since the collisions of opposite-parity pairs cause pair annihilation, the stationary state on the periodic lattice contains all same-parity particles and/or same-propagating-direction particles only. (Notice that only if the size of the lattice is even does the parity have global meaning. If the size is odd, then the parity of a soliton changes every time it travels around the lattice, so that only the latter case is possible.) If there are L_o (L_e) odd (even) left-going solitons and R_o (R_e) odd (even) right-going solitons in the initial state, the stationary state will contain

$$\begin{aligned}
&|L_o - R_e| \quad \text{of odd left-going solitons} \quad &&\text{if } L_o > R_e \\
&|L_o - R_e| \quad \text{of even right-going solitons} \quad &&\text{if } L_o < R_e \\
&|L_e - R_o| \quad \text{of even left-going solitons} \quad &&\text{if } L_e > R_o \\
&|L_e - R_o| \quad \text{of odd right-going solitons} \quad &&\text{if } L_e < R_o
\end{aligned} \tag{5.6}$$

The expectation value of the number of solitons in the random initial con-

figuration can be calculated by adding the product of all triplets in which the middle site is zero times the number of solitons in that triplet. This procedure gives an expectation value of $10N/27$ solitons, where N is the size of the lattice. Additionally, there are some solitons that arise from the $1M$ and $M1$ in the initial configuration. This contribution depends on the specific rule for each subregion, but is always much smaller than the contribution from the zeros; for example, in one of the subphases of the T-phase, the $1M$ and $M1$ add an extra $14N/3^5$ to the expectation value. Some of the solitons will form double walls (solitons traveling in the same direction separated by the minimum distance, see Fig. 7d). The expectation value of the double walls in the initial configuration can be calculated in the same manner and is $4N/3^5$. In the language of particles in the P-I system, each species (specified by the direction and parity) is created with equal probability and the expectation value of each species is $\sim 5N/54$.

The total number of solitons in the stationary state is the fluctuation in the numbers of the solitons of each species. Therefore, assuming random initial conditions, the expectation value of the number of solitons surviving is of order $\sqrt{N}$, so the density is proportional to $1/\sqrt{N}$. In the phase S_a there is also the possibility that some double walls will survive. The probability of any individual double wall surviving is approximately the square of a single soliton surviving. Hence, the probability of there being double walls in the stationary state can then be estimated as $[2(27/10\pi N)^{1/2}]^2(4N/35) \approx 1/20$. This is independent of the system size, so the density becomes of order $1/N$.

The effective rules for the S-phase can now be deduced. For almost every initial condition the stationary state of the S-phase must contain large stretches of homogeneous sites since the density of solitons is proportional to $1/\sqrt{N}$. With probability one for large N, the stationary state must also contain isolated left- and/or right-going solitons. In phase S_a there is also a 1/20 probability that the stationary state will contain double walls. The effective rules in the S_b-phase are as follows: the rules for triplets (000), (111), (MMM) due to homogeneous stretches; the rules for triplets (001), (011), (110), ($0MM$), ($MM0$) due to isolated solitons, with additional rules for ($M01$), ($00M$) for left-going solitons and ($10M$), ($M00$) for right-going solitons. In the S_a-phase there may also be effective rules for (010) and ($0M0$) due to the double walls. The collision between equal-parity particles does not introduce any new rules.

In the T-phase odd-parity collisions do not result in the annihilation of particles, and relative parities between particles are conserved. Therefore odd-parity collisions are present in the stationary state and all triplets occur except for those containing $M1$ or $1M$. Hence the effective local rules are those obtained empirically in Section 3.

6. STATIONARY STATES IN THE LARGE LATTICE LIMIT

We have shown in the preceding section that after two time steps the configurations and dynamics of the T- and S-phases can be mapped by ϕ to an interacting particle system. To consider the stationary state of the particle system, we further map the system to a new particle system (P-II system). Then we will show that both the T- and S-phases have unique observable stationary states. The stationary state for the T-phase spatially defines a Gibbs random field.

6.1. Mapping to Particle System II

From now on we consider infinite systems. Let the particle positions in the P-I system constructed in Section 5 be

$$\cdots y_{-2} \leqslant y_{-1} < 0 \leqslant y_0 \leqslant y_1 \leqslant \cdots \tag{6.1}$$

Mimicking Sinai,[44] we introduce the following map θ:

$$\begin{aligned} &\theta(y_0) = x_0 \\ &\theta(y_i) = x_{i-1} + y_i - y_{i-1} - q(y_i - y_{i-1}), \qquad \text{if} \quad i > 0 \\ &\theta(y_i) = x_{i+1} + y_i - y_{i+1} + q(y_{i+1} - y_i), \qquad \text{if} \quad i < 0 \end{aligned} \tag{6.2}$$

where

$$q(y) = \begin{cases} 4 & \text{if } y \text{ is even} \\ 1 & \text{if } y \text{ is odd} \end{cases} \tag{6.3}$$

We further assign a color, red or blue, to each particle, depending on whether x_i is even or odd. The velocity of the particle at x_i is identical to that of the original particle at y_i. Let $T' = \phi \circ T \circ \phi^{-1}$ be the time evolution operator for the P-I system. $S = \theta \circ T' \circ \theta^{-1}$ defines the dynamics as follows:

1. Unless two particles are at the same site, $x_i = x_i + u_i$, where u_i is the velocity of the ith particle ($u_i = +1$ for right-going particles and -1 for left-going particles).
2. If two particles are at the same site, the colors and indices are exchanged, but the particles pass through one another.
3. When the particle with index zero passes through the origin to the left, the index of each particle is decremented by 1 and the position of each particle is incremented by either 1 or 4, depending on whether the particle immediately to the right is of the same or the opposite color.

4. When the -1 particle passes through either 4 or 1 to the right, depending on whether the particle immediately to the right is of the same or opposite color, the index of each particle is incremented by 1 and the position decremented by either 4 or 1.

The map θ is one-to-one in the sense that $\theta^{-1}\theta = 1$. Since the $0M1$ system and the P-I is one-to-one, so is the relation between $0M1$ and P-II. We consider the phase space $\Omega_2 = \theta \circ \phi(T^2\{0, 1, M\}^Z)$. The Ω_2 is a subset of the set of all possible color-direction combinations of the P-II system. A detailed characterization of Ω_2 follows.

The restrictions on the configuration space of the P-I system place restrictions on the configuration space of the new system. The separation between a particle P and P', the next particle traveling in the same direction, is $4 + 6i$ ($i = 0, 1, 2,...$ for T- and S_a-phases, while $i = 1, 2,...$ in S_b) and is independent of the number of particles traveling in the opposite direction between P and P'. The separation between P and the next particle traveling in the opposite direction is $2i$ ($i = 0, 1, 2,...$) and is independent of the number of particles traveling in the same direction as P between the two particles. There are no restrictions on the sequence of colors. These conditions require that the particles are either on all even or on all odd lattice sites at any one time and that only two particles can occupy any site at once. Therefore, the dynamics of the system is completely specified.

The dynamics under this second map is almost free particle, with the exception for a random walk due to the particles crossing the origin. This is similar to the hard-rod model studied by Sinai,[44] and Aizenmann *et al.*,[43] except there are two species of particles instead of just one.

This mapping is useful in showing that the $N \to \infty$ limit stationary state for the T-phase is a Gibbs state, and also that the T-phase is weakly turbulent (Section 8.3).

6.2. *T*-Phase Exhibits Gibbs Random Field

Let $\Omega_0 = \{0, 1, M\}^Z$ be the phase space of the $0M1$ system. Let μ_0 be the uniform measure on Ω_0 (i.e., the product measure). We topologize Ω_0 by introducing the Tikhonov topology. Note that in this topology $x, y \in \Omega_0$ are close if x and y differ only at remote lattice points from O. Thus, this topology is in conformity with our basic idea on observation.

In Section 5 we have shown that $\Omega_1 = T^2\Omega_0$ can be described as a many-particle system (P-I system). The initial measure μ' for the P-I system is a Gibbs measure. Although the statement is almost trivial, for convenience we will give an explicit proof here. Let $\mu_1 = \mu_0 \circ T^{-2}$, which is a measure on Ω_1. Let $\Lambda \subset Z$ be a finite set on the 1D lattice and $\Lambda^C = Z \backslash \Lambda$

(Z outside of Λ). For $x \in \Omega_1$, x_Λ is the configuration restricted to Λ. We use $x_\Lambda \vee y$ (following Ruelle[5]) to denote the element $\xi \in \Omega_1$ such that $\xi_\Lambda = x_\Lambda$ and $\xi_{\Lambda^c} = y$. A measure μ is a Gibbs measure if the conditional probability satisfies:

1. $\mu(\xi_\Lambda = x \mid \xi_{\Lambda^c} = y)$ is positive iff $x \vee y \in \Omega_1$
2. $\mu(\xi_\Lambda = x \mid \xi_{\Lambda^c} = y)$ is continuous w.r.t. y for each x and Λ

In our case $\mu(\xi_\Lambda = x \mid \xi_{\Lambda^c} = y)$ is always positive if $x \vee y \in \Omega_1$. Therefore we have only to check the continuity. Intuitively, if two portions far apart on the lattice are uncorrelated, then a small change in y (i.e., the change of configuration far away from Λ) should have little effect on the probability of finding x in Λ. But this is obvious from the construction of μ_1; T is defined through local rules f so that, if Λ and Λ' are more than four lattice points apart, then

$$\mu_1(\xi_\Lambda = x, \xi_{\Lambda'} = y) = \mu_1(\xi_\Lambda = x)\, \mu_1(\xi_{\Lambda'} = y)$$

since μ_0 is the uniform product measure on Ω_0. Hence μ_1 is a Gibbs measure.

Next, we map the $0M1$ system after two timesteps to the P-I system by ϕ constructed in Section 5. Let $\Omega_2 = \phi\Omega_1$. Here ϕ is a bijection, and is defined locally, so that ϕ is a morphism in Ruelle's[5] sense. Hence $\mu' = \mu_1 \circ \phi^{-1}$ is again a Gibbs measure.

We use this fact to prove that the observable invariant measure on Ω_2 is a Gibbs measure. We map the P-I system to the P-II system by the map θ introduced in Section 5. Let $\Omega_3 = \theta\Omega_2$. We can topologize Ω_2 and Ω_3 by introducing the Tikhonov topology regarding the whole lattice as the direct product space of cells. Then the map θ becomes continuous: Let $x \in \Omega_2$ and $y = \theta x$. For any neighborhood U_2 of y there is a subset $K \subset Z$ around O such that U_2 contains all the configurations that differ from y only outside K. Then $\theta^{-1}(U_2)$ contains all the configurations that differ from x only outside a subset $K' \subset Z$ whose size is not smaller than the size of K. Hence for arbitrary U_2, we can have an open set $V_1 \subset \theta^{-1}(U_2)$. Hence θ is continuous. Let $\nu = \mu' \circ \theta^{-1}$. Although ν is a Gibbs measure, it is not an invariant measure.

The P-II configuration is specified by the particle and the color configurations, so that $\Omega_3 \subset \Omega_P \times \Omega_C$, where Ω_P is the particle phase space and Ω_C is the color configuration space. Let π_P (π_C) be the projection to Ω_P (Ω_C), and $\nu_P = \nu \circ \pi_P^{-1}$, $\nu_C = \nu \circ \pi_C^{-1}$. These are marginal distributions and it is easy to show $\nu \neq \nu_P \times \nu_C$.

Since on Ω_3, $S \equiv \theta \circ \phi \circ T \circ \phi^{-1} \circ \theta^{-1}$ is reversible (this means that T is also reversible on $\Omega_1 = T^2\Omega_0$), $S^\infty\Omega_3 \equiv \bigcap_{n=1}^{\infty} S^n\Omega_3 = \Omega_3$, i.e., the phase

space is invariant. On this set we claim that the direct product measure $\nu_P \times \nu_C = \nu_\infty$ is the observable invariant measure. Since ν_P and ν_C are Gibbs measures, so is ν_∞.

Let us suppress colors and only consider particle positions in the P-II system. Next, we separate right-going and left-going particles. The particle configuration is a superposition of these right- and left-going particle configurations. They do not interact with each other. Hence, the configuration of the right-going (left-going) particles translates rigidly with an occasional rigid shift due to the color constraints. Since ν_P is obviously translationally symmetric, ν_P is invariant. The same discussion applies to ν_C; ν_C is also invariant.

If we can prove that eventually the correlation between color and position configurations is almost surely lost (w.r.t. ν), then we may claim that $\nu_P \times \nu_C$ is the invariant measure. Its observability in the sense of Section 4 must be proven separately.

Let ν_∞ be the invariant measure. We want to show that for any local finite cylinder set $\beta \subset S^\infty \Omega_3 \equiv \bigcap_{n=0}^{\infty} S^n \Omega_3$

$$\nu_\infty(\beta) = \nu_P(\beta)\, \nu_C(\beta) \tag{6.4}$$

Then this implies $\nu_\infty = \nu_P \times \nu_C$. Let β be a set of configurations on a finite set Λ. As can easily be seen, each particle p_i travels with average velocity u_i while the color lattice shifts $O(\sqrt{t})$. After time t the color lattice shifts $n_{\text{right}}(t)$-$n_{\text{left}}(t)$, where $n_{\text{left(right)}}(t)$ is the number of particles traveling through the origin to the left (right) during time t. Since the measure ν is symmetric under space reversal and n_{left} and n_{right} are proportional to t, the difference is ν-almost surely $O(\sqrt{t})$. Each particle p_i travels $tu_i + c(n_{\text{left}} - n_{\text{right}})$, where $|c| < 4$. Therefore the average velocity of p_i is $u_i + O(1/\sqrt{t})$.

Notice that the correlation between colors and particle positions exists only within the range of two lattice points with respect to the measure ν. As we have already seen, with ν-probability 1 the subsets of the lattice occupied by the same configuration and by the same color pattern are separated by $O(N)$ lattice points after N time steps. Hence on any subset of the lattice whose size is less than bN, where b is an appropriate positive constant, the color and particle position patterns are statistically independent. Let $\nu_N = \nu \circ S^{-N}$. Then for any cylinder set β of configurations on any finite subset Λ of the lattice whose convex hull has diameter smaller than bN, we have

$$\nu_N(\beta) = \nu_C(\beta)\, \nu_P(\beta) \tag{6.5}$$

Let us consider the family of measures $\{\nu_N\}_{N=1}^{\infty}$. Since the set of all

measures on Ω_3 is a compact set (with the weak topology), $\{\nu_N\}_{N=1}^{\infty}$ has an accumulation point. Let us denote this to be ν_∞. By construction

$$\nu_\infty(\beta) = \nu_C(\beta)\,\nu_P(\beta) \tag{6.6}$$

for any set of local configurations on any finite subset of the lattice. Hence $\lim_{N\to\infty} \nu_N$ is unique and identical to $\nu_C \times \nu_P$.

Finally we show that ν_∞ is observable. After two time steps again we can map any finite system to a finite P-II system with minor technical modifications. Let N be the size of the system. Then after about each N time steps the correlation between color and configuration reappears. However, this correlation lasts only a few time steps (definitely independent of N). Hence, if we make statistical tables of cylinder sets, asymptotically in the $N\to\infty$ limit, they correspond to independent color–configuration statistics. Obviously, the finite lattice configuration distribution and color distribution converge, respectively, to ν_P and ν_C. Therefore, $\nu_P \times \nu_C$ is an observable invariant measure. In this case it is unique.

Y. Takahashi (private communication) has conjectured that all the observable stationary states of 01-CA are Gibbs random states.

The observable measure obtained for the T-phase is a K-measure. We believe that this is, however, not Bernoulli, since the P-II system is similar to a system known to be K but not Bernoulli. The system is given as follows. Let σ be the full shift on $X \equiv \{-1, 1\}^Z$ with uniform measure μ. Let $x = \{x_n\}_{-\infty}^{+\infty}$ and $y = \{y_n\}_{-\infty}^{+\infty}$, where $x, y \in X$. Put $R(x, y) = (\sigma x, \sigma^{x_0} y)$. Then $R(x, y)$ has been shown by Kalikow[45] to be K but not Bernoulli. In the P-I representation, we have left and right particle lattices, which basically undergo a shift, and the color lattice, which shifts left or right, depending on the value of the particle lattices near the origin. The measures on the left and right lattices are the same.

There are other examples of non-Bernoulli K-systems, but as far as we know, all these examples[45] are designed to be non-Bernoulli. We may say that our T-phase would be the first non-Bernoulli K-system that was not explicitly created as a counterexample. We will return to this problem in a following paper.

6.3. S-Phase Is Trivial

We have shown in Section 5.4 that the density of solitons in the S-phase is asymptotically $1/\sqrt{N}$, where N is the size of the lattice. Therefore a local observer would see fewer and fewer solitons (or particles in the P-I representation), until finally in the $N\to\infty$ limit no soliton will pass the origin during any finite time observation. Hence, to the observer

the stationary state is purely homogeneous (i.e., the homogeneous states have measure 1 with respect to the observable invariant measure) and the S-phase is trivial.

7. POSSIBLE CHARACTERIZATION OF "TURBULENT" PATTERNS

We have analyzed the T- and S-phases in detail in the preceding sections. In the large-system limit the S-phase is trivial. The T-phase in this limit gives a Gibbs random field corresponding to disordered statistical systems. Although this is a very nice property, it is clear from the simple counterexamples discussed previously that this does not necessarily imply that the system exhibits turbulent space-time patterns. The T-phase has been mapped to an "almost" independent particle system, system P-II, but in this system, in contrast to ideal gas systems, the effect of localized perturbation affects increasingly many particles (hence, in the original system, many cells). This propagation property of disturbances is not found in the simple counterexamples. As is suggested by Wolfram,[19] this propagation property should be required in order to have turbulent space-time patterns. However, as we will see later, there are difficulties in this proposal.

Before going into our own proposal in the next section, here we critically survey possible characteristics of "turbulent" states.

Attempts so far to characterize complicated space-time patterns may be summarized as follows. Wolfram[19] introduced space and time entropies and the Kolmogorov–Sinai entropy with respect to a special partition, and used them to try to characterize "classes I–IV" of CA. He also introduced a Green's function to characterize the propagation of the effect of perturbation applied to a cell at time t. Packard[20] introduced the Liapunov characteristic (LC) exponent, which is the usual LC exponent for the dynamical system on S introduced in Section 4. If there is a propagation of patterns (i.e., if Wolfram's Green's functions have domains that expand linearly in time), then the LC exponent becomes positive. Moreover, it should be noted that, if the system has a positive Kolmogorov–Sinai entropy, we can always invent a metric that gives us the LC exponent identical to the entropy. Thus, the LC exponent is not a distinct quantity.

We consider the following possible characteristics of turbulent space-time configurations:

1. Complexity
2. Positivity of entropies
3. Decay of space-time correlation functions

4. Length of period as a function of system size
5. Sensitive dependence on initial conditions
6. Relation to random fields

Although it is almost immediately obvious that 1–3 and 6 are insufficient, they are still of some interest, so we include here some general discussion of these characteristics. Item 5 is closely related to Wolfram's proposal; we will point out its inherent difficulty.

7.1. Complexity of Patterns

Intuitively, we expect that turbulent patterns should be complicated, so we must make the meaning of complication or complexity clear. As is mentioned in the introduction, the definition of randomness is directly related to the definition of algorithmic complexity.[16] Hence, even in our present case of space-time patterns, it may be reasonable to use complexity in the algorithmic sense. It is reasonable to define complexity of the stationary state on a size N lattice as the minimum program length for a universal Turing machine[46] to produce the space-time pattern. If the necessary program is asymptotically the size of order NT for large N, where T is the period, we say that the stationary state is algorithmically complex. In this definition all the patterns are converted into 1D strings, so that we can use an ordinary Turing machine. The definition is in conformity with that for the complexity of sequences.[16,18] We have the following obvious, but nonetheless important proposition:

Any nontrivial stationary state of CA cannot be algorithmically complex. Here "nontrivial" implies that the period is an increasing function of the system size without upper bound.

Proof. Let $S_{\mathbf{a}}(N)$ be the periodic orbit for the finite lattice size N with the initial configuration $\mathbf{a} \in A^N$. To specify $S_{\mathbf{a}}(N)$, we must specify $T_N = \# S_{\mathbf{a}}(N)$ (the period) times N cell states. However, to produce this pattern, we only need N and the initial condition $\mathbf{a} \in A^N$. The dynamics and the program to find the period by pattern matching require only a finite-length program with length independent of N; asymptotically we need only of order N bits of source program for a Turing machine. Hence, the ratio of program length divided by NT goes to zero asymptotically due to the nontriviality. ∎

Notice that the proposition is true even if the local rules are absolute cell-position-dependent.

Wolfram[19] concluded an analogous statement, "the evolution of CA can never generate random space-time pattern," from the construction of

the configuration entropy of the space-time pattern. The assertion, as well as the above proposition, is really trivial. However, this implies that it is highly likely for us visually to recognize significant (meaningful) patterns in the space-time configuration of CA. In these patterns, however, *no* deep physical or mathematical facts need be involved; they must appear due to the deterministic nature of the model itself.

Thus, if we require the complexity of a space-time pattern to be a characteristic of "turbulent" patterns, then no CA can be turbulent. However, we still believe that certain patterns produced by CA are sufficiently complicated, reminding us of turbulence. To characterize these patterns, the above observation shows that the algorithmic randomness is useless.

Even if the space-time patterns are truly complex in the algorithmic sense, the system need not be entitled to be called turbulent. Consider a very trivial system: juxtaposed maps, i.e., the CM without any spatial coupling. If each map is chaotic, then we can have, in the genuine sense, complex space-time patterns. However, any spatially localized perturbation cannot, by definition, propagate to cause global disturbances; the system is almost stable. It is not at all sensible to call such a system turbulent. Hence, we must conclude that the algorithmic complexity is neither sufficient nor necessary to characterize turbulence.

Thus, we will not consider the algorithmic complexity of space-time patterns further. There are other measures of complexity, some[24] of which are interesting, but they try to measure subtle organization of patterns, so we will not consider them here.

7.2. Entropies

7.2.1. Kolmogorov–Sinai Entropy. The positivity of the Kolmogorov–Sinai entropy is not a sufficiently strong characteristic to distinguish turbulent space-time patterns, as is clear from examples A–C in Section 3. There is a fundamental objection to the Kolmogorov–Sinai entropy as an indicator of turbulent patterns. As is noted in the introduction, isomorphisms do not respect any spatial structure, so that isomorphism invariants cannot be used to characterize turbulent space-time patterns. Hence, the Kolmogorov–Sinai entropy must be disqualified as an indicator of turbulent patterns. However, still the KS entropy is an interesting quantity, so here we mention a few generalities on this quantity.

The relation between the complexity and the dynamical theoretical entropies due to Brudno[18] suggests that the Kolmogorov–Sinai entropy of any CA is bounded from above even in the infinite-system-size limit. Wolfram[19] defined and showed the finiteness of a lower bound of the

Kolmogorov–Sinai entropy for 1D CA by choosing a special partition of A^Z, i.e., the partition $\{[a], a \in A\}$, which is, in general, not a generator.

If the state of the ith cell at time $t+1$ is determined by the states of cells at time t in a finite set $\mathcal{N}_i$ ($\mathcal{N}_i \ni i$) for all $i \in L$, we say the CDS is a local CDS (LCDS), where $\#(\mathcal{N}_i)$ is uniformly bounded from above by $\mathcal{N}$. If a LCDS allows only a finite cell state set, we call it a local CA (LCA). Ordinary CA are all LCA. The local rules may be spatially inhomogeneous, i.e., the rules can depend on the absolute positions of cells. For LCA we have the following proposition:

Any LCA has a finite Kolmogorov–Sinai entropy for any T-invariant empirical measure (constructed in Section 4).

Proof. (For simplicity, a proof for a 1D system is given.) The measure-theoretic entropy is defined as[26]

$$h_\mu(T) = \sup_{\mathscr{B}} h_\mu(T, \mathscr{B}) \tag{7.1}$$

where $h_\mu(T, \mathscr{B})$ is the entropy of T with respect to the partition $\mathscr{B}$, and sup is taken over all finite partitions of A^Z. First, we use the standard fact that A^Z can be mapped to $S = [0, 1] \times [0, 1]$, as has already been done in Section 4. Any finite partition on A^Z is represented by a finite partition of S. In this representation any cylinder set around the observer corresponds to a rectangle. Notice that minus log of the area of the rectangle is asymptotically proportional to the length of the word necessary to specify the cylinder set. If any member of the partition $\mathscr{A}$ is a finite sum of finite-length cylinder sets, then $h_\mu(T, \mathscr{A})$ is finite. For such $\mathscr{A}$, each component is characterized by words of length less than, say, l (we call such a partition an l-local partition). Due to the definition of LCA, we have the following estimate:

$$\#\left(\bigvee_{i=0}^{n} T^{-i}\mathscr{A}\right) \leqslant (\#A)^{n\mathcal{N}+l} \tag{7.2}$$

so that $h_\mu(T, \mathscr{A}) \leqslant \mathcal{N} \log(\#A)$. We can always make a monotonically refining sequence of local partitions $\{\mathscr{A}_n\}$ converging to an arbitrary partition which is measurable by experimentally accessible measures. Then the mutual entropy $H(\mathscr{B} \mid \mathscr{A}_n)$[26] of the partitions $\mathscr{A}_n$ and $\mathscr{B}$ converges to zero. We know the inequality[26]

$$h_\mu(T, \mathscr{B}) \leqslant h_\mu(T, \mathscr{A}_n) + H(\mathscr{B} \mid \mathscr{A}_n) \tag{7.3}$$

but $h_\mu(T, \mathscr{A}_n)$ is uniformly bounded. Hence $h_\mu(T, \mathscr{B})$ must also be finite for any finite partition $\mathscr{B}$ that is measurable by empirical measures. ∎

We do not claim that the finiteness of entropy is always true for any invariant measures. The logic used in the proof is not necessarily legitimate for pathological measures that are not empirically obtainable.

If there is no propagation of patterns, then the topological entropy of the system is zero. However, the converse is not true. We can easily make a LCA for which the pattern propagates with velocity asymptotically proportional to $1/t$.

Our consideration implies that any LCA has zero entropy density. This is in conformity with our complexity consideration in the preceding subsection. It should be noted that there is a marked difference between finite-state LCA and, for example, the Navier–Stokes equation, for which Ruelle and others (e.g., Ref. 16) have suggested that there is a positive entropy density. Thus, at least mathematically, there is a fundamental difference between finite-state LCA and systems governed by partial differential equations. We do not know how serious the difference is from the physicists' point of view. The difference seems similar to the difference between rational numbers and irrational numbers; they are fundamentally different, but, for practical purposes, there is almost no difference.

7.2.2. Sequence Entropies. Wolfram[19] used the combinatorial entropies along the time direction ($i = \text{const}$) and along the spatial direction ($t = \text{const}$). We can introduce the combinatorial entropies along any direction in the space-time (or we can even consider entropies along curves). Let $\{S_i\}_{i=0}^{\infty}$ be a sequence of cell states along a line (precise specification of the line is not important). The entropy h per symbol of this sequence is defined as follows. Let $p_j^{(i)}$ be the relative frequency of the jth (according to some lexicographic order) sequence consisting of i symbols. Then we set

$$h = \lim_{i \to \infty} \sup \left(-\frac{1}{i} \sum_j p_j^{(i)} \ln p_j^{(i)} \right) \tag{7.4}$$

(recall the Shannon–MacMillan–Breiman theorem[47]). If the sequence is taken along the line parallel to the time axis, h gives the lower bound to the Kolmogorov–Sinai entropy of the system. Since the sequence of cell states in front of the observer must be chaotic, h along the time axis must be positive. Can we then say that the pattern is turbulent, if both the entropies in time and space directions are positive? Example C provides us with a negative answer to this question. Actually, the example has positive entropy along any line in space-time. Hence, we must conclude that the positivity of sequence entropies is not sufficient to characterize turbulent patterns.

7.3. Other Properties

7.3.1. Decay of Space-time Correlations. Let $s(n, t)$ be the state of cell n at time t, which is a number according to a suitable encoding scheme. Then we can define the space-time correlation as

$$C(n, t) = [\langle s(n, t)\, s(0, 0)\rangle - \langle s(0, 0)\rangle^2]/\langle s(0, 0)\rangle^2 \tag{7.5}$$

where $\langle\ \rangle$ is the ensemble average with respect to an invariant measure. To be chaotic, $C(n, t)$ must decay (but need not decay to zero). If $C(n, t)$ decays in any space-time direction, the space-time pattern may be turbulent. However, again for example C, $C(n, t)$ decays in any space-time direction. Hence, we must conclude that the decay of correlation functions is not an adequate property to characterize "turbulent" patterns.

7.3.2. Length of Period As a Function of System Size. To have positive entropy the period T_N cannot be a bounded function of the system size N. One might suggest that exponentially increasing T_N with N characterizes "turbulent" patterns. We hesitate to support this suggestion. Suppose the sequence of cell states parallel to the time axis is statistically homogeneous in time. From the consideration given in the argument for complexity, we need only of order N symbols to specify the periodic orbit of length T_N. Hence, if there is $a > 0$ such that T_N is $\sim e^{aN}$, then the complexity per letter must be exponentially small. That is, the orbit must be organized in a very delicate way to extend the period, so that the sequence must be highly organized. Thus, we hesitate to use T_N to characterize turbulent patterns.

7.3.3. Sensitive Dependence on Initial Conditions. This is an intuitively appealing property to consider, but we first must point out that completely decoupled CM with chaotic maps considered in Section 7.1, which we preferred not to regard as turbulent, would be turbulent under this definition. Therefore the sensitivity is not sufficient, because sensitivity does not, in general, exclude systems without the propagating property. Moreover, there is a theoretical (and practical) difficulty. We want to characterize a dynamical system with an invariant measure (i.e., stationary states), and in the context of the usual theory of chaos, we do not consider perturbations that take the initial conditions outside the attractive basin of the invariant measure. Unfortunately, we do not know how to perturb initial conditions while still keeping the system in the same basin of the stationary state.

If we naively assume that many local perturbations do not destroy the stationary state, then the propagation of the effect of the localized perturbation, which can be studied by the increase of the Hamming distance $H(t)$

between the unperturbed and the perturbed systems, as has been proposed by Wolfram,[19] might be a good measure of sensitivity to the perturbation. However, there is a counterexample. Consider our S-phase in model $0M1$. The invariant measure concentrated on the 3-cycle $\{*0*, *M*, *1*\}$ is orbitally stable against any local perturbation, but many local perturbations can produce propagating disturbances [$H(t)$ often increases linearly in time]. (Recall that the S-phase is an analogue of the excitable state in the Belousov–Zhabotinsky system.[36,37])

Thus we must conclude that so far no satisfactory measure of sensitivity has been proposed.

7.3.4. Relation to a Stochastic Field. As is discussed in the introduction, chaos is closely related to stochastic processes. Since the complexity of space-time patterns of any LCA is zero, there is no way to have a natural relation between the space-time pattern of CA and space-time random fields.

However, if we consider only the spatial pattern, we can have a natural relation to random fields. For example, as we have shown, our T-phase exhibits spatial patterns obeying a Gibbs random field. But a stochastic field is quite insufficient to characterize turbulent space-time patterns. We only need to consider the examples in Section 4.2 to see this.

8. WEAK TURBULENT PHASES

In the preceding section, we have shown that many intuitively appealing quantities are insufficient or disqualified as characteristics of "turbulent" space-time patterns. We believe, as Wolfram did, that randomness of patterns and sensitivity of the global pattern to local disturbances are essential to characterize turbulence. However, as we will show at the end of Section 8.2, these properties are still insufficient. Therefore we consider the complicatedness of the generating partition of the system. A quantitative measure of this complicatedness, P-entropy, is introduced. We would like to call systems with positive P-entropy weakly turbulent. Then we show that the T-phase is weakly turbulent. The reason we add "weakly" is that we expect stronger turbulence to be possible in CM and PDE systems; they may have positive entropy density (or even positive P-entropy density), in contrast to CA.

8.1. Motivation

If many similar spatial structures in the t-time-step past of the cell O can give different states at $t=0$ for the cell O, we would have difficulty in

discerning the regularity. The origin of this difficulty lies in the incompatibility of the two partitionings of the state space (in our case, A^Z): one based on the dynamics and the other based on the spatial (visual) patterns. By "incompatibility" we mean the following: spatially similar patterns belong to different elements of partitions generated by a generator of the dynamical system (similarity of patterns is measured according to a suitable norm). More informally, if partitionings of the state space according to the spatial pattern in the present and according to that in the distant past (or future) are quite different (almost independent), we will have a great deal of difficulty in discerning the space-time regularity. We believe this is the essence of the turbulent space-time patterns.

In the following preliminary attempt we take CA as an example and make what we have outlined more quantitative.

8.2. *P*-Entropy

Let us introduce a suitable distance $\|\cdot\|_D$ between spatial patterns. Let $\omega, \omega' \in A^Z$. We define

$$\|\omega - \omega'\|_D = \mathrm{Max}\{i \mid \omega_i \neq \omega_i'\} - \mathrm{Min}\{i \mid \omega_i \neq \omega_i'\} \tag{8.1}$$

i.e., $\|\omega - \omega'\|_D$ is the size of the smallest connected subset of the lattice outside of which ω and ω' are identical. Let us call this distance the *discrepancy distance*. We define the discrepancy distance between two sets A and B by

$$\rho_D(A, B) = \inf\{\|\omega - \omega'\|_D, \omega \in A, \omega' \in B\} \tag{8.2}$$

To be specific we consider 1D finite-state LCA $T: A^Z \to A^Z$ with an observable invariant measure μ (i.e., constructed according to the prescription of Section 4) on an invariant set $\Omega \subset A^Z$. Let $\mathscr{A}$ be a local partition of Ω. From this partition we generate the following partition:

$$\mathscr{A}_N = \bigvee_{i=0}^{N} T^{-i}\mathscr{A} \tag{8.3}$$

Any element of this partition is a subset of an element of the partition $\mathscr{A}$.

The Dc-hull of $p \in \mathscr{A}_N$ is a subset of $\mathscr{A}_N$ such that

$$[p]_c = \{p' : \rho_D(p', p) \leqslant c, \mu(p') > 0, p' \in \mathscr{A}_N\} \tag{8.4}$$

We define

$$n_{N,c}(p) = \#\{p' : p' \in [p]_c, p' \in \mathscr{A}_N, T^N p' \cap s = \varnothing \text{ if } T^N p \subset s \in \mathscr{A}\} \tag{8.5}$$

That is, we count the number of elements of the partition $\mathscr{A}_N$ that is discrepancy distance c close to the element p but does not give the same element of $\mathscr{A}$ after N time steps. The number is a measure of the incompatibility of pattern-based and dynamics-based partitions around p (see Fig. 8 for a more intuitive explanation).

We would like to modify the definition of the Kolmogorov–Sinai entropy taking into account only those elements of the partition $\mathscr{A}_N$ with large $n_{N,c}(p)$, say, $n_{N,c}(p) \geqslant \beta N$ for some positive constant β. That is, we take into account the elements of $\mathscr{A}_N$ which have "complicated shapes" with respect to the topology based on the visual similarities of the local patterns (see Fig. 8).

The P-entropy $P\text{-}h_\mu(T, \mathscr{A}, \beta, c)$ with the threshold β with respect to the T-invariant measure μ, the local partition $\mathscr{A}$, and discrepancy c is defined as follows:

$$P\text{-}h_\mu(T, \mathscr{A}, \beta, c) = \lim_{N \to \infty} \sup - \sum_{\substack{p \in \mathscr{A}_N \\ n_{N,c}(p) \geqslant \beta N}} -\mu(p) \ln \mu(p) \tag{8.6}$$

If we set $\beta = 0$, (8.5) reduces to the ordinary Kolmogorov–Sinai entropy $h_\mu(T, \mathscr{A})$ with respect to the partition $\mathscr{A}$. If $h_\mu(T, \mathscr{A})$ is finite, then the

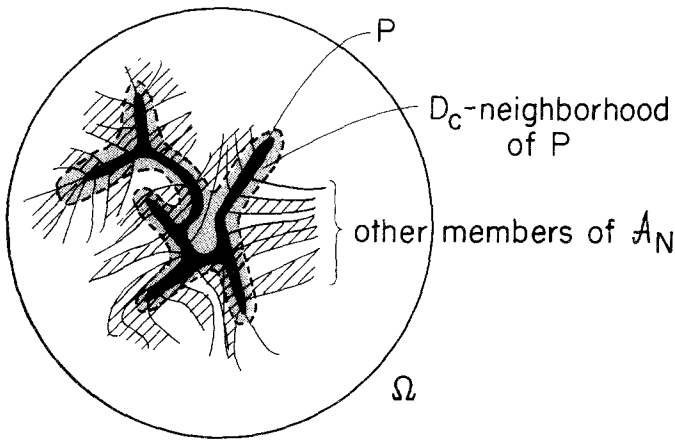

Fig. 8. Each element of $\mathscr{A}_N$ is the set that can give a specific time evolution around O during N time steps. Let us take an element $p \in \mathscr{A}_N$ (the black area) and consider its neighborhood defined as the totality of spatial patterns locally similar to the patterns exhibited by elements in p (shaded area). $[p]_c$ is the totality of elements in $\mathscr{A}_N$ overlapping with the neighborhood of p. The $n_{N,c}(p)$ is the number of elements of $\mathscr{A}_N$ in $[p]_c$ that gives different elements of $\mathscr{A}$ than that given by p after N time steps (hatched elements). If there are many such elements, we will not be able to predict the future local patterns of the system readily.

P-entropy is a bounded, nonnegative, decreasing function of β, so that the following limit exists:

$$\lim_{\beta \to 0} P\text{-}h_\mu(T, \mathscr{A}, \beta, c) = P\text{-}h_\mu(T, \mathscr{A}, c) \tag{8.7}$$

which we call the P-entropy with respect to the partition $\mathscr{A}$ and discrepancy c.

The P-entropy is defined as

$$P\text{-}h_\mu(T, c) = \sup_{\mathscr{A}} P\text{-}h_\mu(T, \mathscr{A}, c) \tag{8.8}$$

where sup is taken over all the local finite partitions of Ω. We have the following obvious but important inequalities for any $c \geqslant 0$:

$$P\text{-}h_\mu(T, c) \leqslant h_\mu(T) \tag{8.9}$$

and if $c_1 > c_2$, then

$$P\text{-}h_\mu(T, c_1) \geqslant P\text{-}h_\mu(T, c_2) \tag{8.10}$$

The following is our (at least tentative) proposal:

Definition. A LCA with positive P-entropy for some finite discrepancy c is said to exhibit *weak turbulent* space-time patterns (or simply weak turbulent).

Inequality (8.9) tells us that weak turbulence implies chaos.

It is possible to define the P-entropy density. We are tempted to define true turbulent patterns by the positivity of this quantity. Recall that we have pointed out that the positivity of the Kolmogorov–Sinai entropy density is not sufficient. We will return to this problem in subsequent papers.

We must show that the definition captures what we want.

We can easily show that the positivity of P-entropy excludes examples discussed in Section 4.2. For example, in the case of the shift, for any local partition $\mathscr{A}$ and for any positive β, there is no summand in the definition of $P\text{-}h_\mu(T, \mathscr{A}, \beta, c)$ for sufficiently large N and any finite c. Hence the P-entropy vanishes.

We next show that P-entropy is not an isomorphism invariant. Although this should be fairly obvious from its definition, we show this by a counterexample. In the stationary state of the T-phase, T is invertible and the Kolmogorov–Sinai entropy is positive finite. Hence, according to Krieger,[48] the system has a finite generator, so that there is an

isomorphism to a shift dynamical system with finite symbols (not necessarily Bernoulli). For this shift system, the P-entropy trivially vanishes, as we have just seen. However, as we will show in Section 8.3, the P-entropy of the T-phase is positive.

We have the following proposition for the positivity of the P-entropy:

Let a LCA, $T: A^Z \to A^Z$, be with a T-invariant ergodic measure μ and local partition $\mathscr{B}$ such that $h_\mu(\mathscr{B}) > 0$. Suppose for some positive β that there is a positive number δ independent of N such that

$$g_{N,c}(\mu, \mathscr{B}, \beta) = \mu(\{p: n_{N,c}(p) > N\beta,\ p \in \mathscr{B}_N\}) > \delta > 0 \tag{8.11}$$

where $\mathscr{B}_N = \bigvee_{n=0}^{N} T^{-n}\mathscr{B}$. Then the LCA exhibits weak turbulence.

Sketch of Proof. According to the Shannon–McMillan–Breiman theorem,[47] asymptotically most of the elements in $\mathscr{B}_N$ have measures of order e^{-Nh}, where $h = h_\mu(T, \mathscr{B})$, so that

$$P\text{-}h_\mu(T, \mathscr{B}, \beta', c) \geqslant \delta h_\mu(T, \mathscr{B}) \tag{8.12}$$

Hence $P\text{-}h_\mu(T, \mathscr{B}) > 0$. ∎

Notice that if we have an infinite sequence $\{N_i\}$ such that $g_{N_i,c}(\mu, \mathscr{B}, \beta) > \delta$ we can still make the same conclusion, since P-entropy is defined by a limit sup in Eq. (8.6).

Intuitively, it would seem probable that the linear increase in time of the width of support of the Green's function (as defined by Wolfram) and positive spatial entropy implies weak turbulence. However, we can make a simple counterexample: Let each cell state be specified by the pair (a_i, ω_i). Let $\{\omega_i\} \in \{0, 1\}^Z$ and define a mapping such that this sequence is stationary (frozen) under the mapping. Let $\{a_i\} \in \{0, 1, M\}^Z$ obey the rule for one of our S-phases. Then in the stationary state, trivially the spatial entropy is $\log 2$, and the width of support of the Green's function (in the sense of Wolfram's) increases linearly in time for "many" perturbations. However, the system has zero Kolmogorov–Sinai entropy in the stationary state, so that it cannot be weakly turbulent. [Notice that in the propositions above, $n_{N,c}(p)$ counts only perturbations that can make naturally occurring cylinder sets. In the S-phase any Hamming distance one perturbation destroys the spatial uniformity, so no such perturbation is admissible.]

8.3. T-Phase Is Weakly Turbulent

The T-phase is weakly turbulent. This can be guessed from the dynamics of the P-I system, which is essentially that of a two-species hard-

rod system. To show the weak turbulence of the model, it is sufficient to show the positivity of the Kolmogorov–Sinai entropy $h_\mu(T)>0$ and $g_{t,1}(\nu_\infty, \mathscr{A}, \beta)>\delta$ for a generator $\mathscr{A}$. The positivity of P-$h(T, 1)$ is then guaranteed by the proposition given in the previous section.

It is easy to show that $h_\mu(T)>0$ in the P-II representation. The observable invariant measure ν_∞ is a direct product measure $\nu_P \times \nu_C$. Let us consider a factor system taking account of the particle motion only. Then this is essentially a double shift. Since ν_P preserves the configuration in $T^2\{0, 1, M\}^Z$, obviously the spatial entropies of the right- and left-going particles are positive. Hence, the Kolmogorov–Sinai entropy of the factor system is positive. This implies that h_ν in the original system is also positive. Thus, it is only necessary to show that $g_{t,1}(\nu_\infty, \mathscr{A}, \beta)>\delta$. In fact we will show a stronger statement: Let $\mathscr{A}$ be a local partition of the P-II system. For $p \in \mathscr{A}_t$ with ν_∞-probability 1, $n_{t,c}(p)>\beta t$ for some finite β. This automatically implies $g_{t,1}(\nu_\infty, \mathscr{A}, \beta)=1$.

The particles travel a distance $t+O(\sqrt{t})$ after t time steps, so that a right-going particle at time t is approximately t sites to the left at time 0 and a left-going particle approximately t sites to the right at time 0. On the other hand, the color lattice has only shifted $O(\sqrt{t})$ in that time span. Therefore, an element $p \in \mathscr{A}$, in general, consists of cylinder sets of length $2t$ on the particle lattice, but only $O(\sqrt{t})$ long cylinder sets on the color lattice.

We consider discrepancy distance one perturbations (which is also the Hamming distance one perturbations) in the $0M1$ model. Any element in the $D1$ hull of a given spatial pattern exists as long as no adjacent M and 1's are contained in the element. There are three methods to make an element in the $D1$ hull: the translation of a soliton by one site and the addition or subtraction of a neighboring pair of solitons. In the P-II representation these correspond to changing the color of a particle and the addition or subtraction of two particles traveling in opposite direction with different colors and separated by 0, 2, or 4 sites. Note that the addition or subtraction of a pair of particles will result in the lattice further away from the origin (than the pair) being translated either toward (if addition) or away (if subtraction) from the origin. The effect of this translation may be canceled on one of the lattices by a change in the number of particles passing through the origin, but if this happens, the particles traveling in the other direction will be shifted from where they were previously. Therefore, at least one of the particle lattices (left- or right-going) will not be at the same position after t time steps. Since the spatial entropy is positive definite, there is a finite probability (independent of t) such that $T^t p'$ is in a different element of $\mathscr{A}$ than $T^t p$ (where p' is an element such that $p' \cap [p]_{D,1} \backslash p \neq 0$). Since the elements of $\mathscr{A}_t$ consist of cylinder sets of

length $2t$, the number of these perturbations grows linearly with t. Hence, for almost every $p \in \mathscr{A}$, $n_{t,1}(p)$ also grows linearly with t and the P-entropy is positive definite.

The other perturbation can be ignored, since changing the color of a particle will only affect the configuration after t time steps if it is on the $O(t)$ points on the color lattice that goes through the origin.

8.4. The 1D Game of Life Is Weakly Turbulent

The 1D game of life is a 1D nearest neighbor CA with the following local rule:

$$f(a, b, c) = \begin{cases} 0 & \text{if } a = c, \\ 1 & \text{if } a \neq c, \end{cases} \qquad a, b, c \in \{0, 1\} \tag{8.13}$$

This is the 01-CA number 90. Topological dynamical aspects have been studied extensively by Martin *et al.*[49] Measure-theoretic aspects, which we are interested in, have been studied completely by Miyamoto[25] (and Kamae, cited in Ref. 25). He has shown that, in our terminology, the observable invariant measure is unique and is the uniform measure ν, so that it is a Gibbs random field. The stationary dynamics is isomorphic to the Bernoulli system $B(1/2, 1/2)$.

Here we show that the 1D game of life is weakly turbulent. Let $A_\alpha = \{\omega : \omega_0 = \alpha, \ \omega \in \{0, 1\}^Z\}$ and make a partition $\mathscr{A} = \{A_0, A_1\}$. Then $h_\nu(T, \mathscr{A}) > 0$, since the system is K. Consider

$$\mathscr{A}_{2^n-1} = \bigvee_{i=0}^{2^n-1} T^{-i}\mathscr{A} \tag{8.14}$$

Then for $N = 2^n - 1$, $n_{N,1}(\nu, \mathscr{A}) = 2^n \sim N$, $\forall p \in \mathscr{A}$. Hence we have positive P-entropy.

9. SUMMARY

Using a caricature model of chemical turbulence, we have studied the infinite-lattice limit of cell dynamical systems.

First we considered the infinite-lattice limit of cell dynamical systems and defined the observability of the asymptotic behavior. Our chemical turbulence model exhibits two different phases at intermediate strengths of coupling constant. One of them, which we labeled T, exhibits apparently random space-time patterns. We showed that the T-phase has a unique observable stationary state in which the spatial pattern is characterized by

a Gibbs random field. In this system macroscopic rules can be predicted from the microscopic rules. We believe that the T-phase is K, but not Bernoulli.

To characterize the T-phase further, we considered the characterization of turbulent space-time patterns critically. We concluded that many candidates, such as the algorithmic complexity, are not sufficient to characterize turbulent patterns. We believe that the essence of turbulent space-time patterns lies in the "incompatibility" of the pattern-based partition and the dynamics-based partition. We proposed a tentative measure, which we called the P-entropy, to characterize this incompatibility and proposed a working definition of weak turbulence. We then showed that both the T-phase of the chemical turbulence model and the 1D game of life are weak-turbulent.

A more detailed analysis of the above-mentioned incompatibility is desirable. We believe that dynamical theoretical analyses of simple CA should be conducted at least at the level of the present paper. So far only the 1D game of life has been analyzed completely.

APPENDIX A. CONSTRUCTION OF MEASURE-THEORETIC CELL DYNAMICAL SYSTEMS

Definition 1. Let A be a finite set, whose element is called a cell state, and a map $f: A^3 \to A$, which defines a local rule of the CDS. A 1D, nearest neighbor, finite state CA on the finite lattice of length N (a positive integer) is a dynamical system (T, A^N), where $T: A^N \to A^N$ is an endomorphism of A^N such that

$$T: (a_0, \ldots, a_{N-1}) \to (a'_0, \ldots, a'_{N-1}), \qquad a_i, a'_i \in A \tag{A.1}$$

with

$$a'_i = f(a_{i-1}, a_i, a_{i+1}), \quad 0 \leqslant i \leqslant n-1, \qquad a_N = a_0, \qquad a_{-1} = a_{N-1} \tag{A.2}$$

The CA (T, A^N) may also be specified as (f, A, N). An element of A^N is called a configuration.

Definition 2. A 1D, nearest neighbor CA is a (topological) dynamical system (T, A^Z), where $T: A^Z \to A^Z$ is an endomorphism of A^Z such that

$$T\{a_i\}_{i=-\infty}^{+\infty} = \{a'_i\}_{i=-\infty}^{+\infty}, \qquad a_i, a'_i \in A \tag{A.3}$$

with

$$a'_i = f(a_{i-1}, a_i, a_{i+1}), \qquad i \in Z \tag{A.4}$$

Definition 3. Let $\mathbf{a}, \mathbf{b} \in A^N$. We write

$$\mathbf{a} \mapsto \mathbf{b} \text{ if and only if } \exists n \in Z^+ \text{ such that } T^n\mathbf{a} = \mathbf{b} \tag{A.5}$$

The *stationary state* $S_{\mathbf{a},N}$ with the initial configuration $\mathbf{a} \in A^N$ is the following set:

$$S_{\mathbf{a},N} = \{\mathbf{b}: \mathbf{a} \mapsto \mathbf{b}, \mathbf{b} \mapsto \mathbf{b}, \mathbf{b} \in A^N\} \tag{A.6}$$

that is, the periodic ω-limit set that can be reached from initial configuration $\mathbf{a}$. The cardinality of $S_{\mathbf{a},N}$ is the period of the cyclic orbit $\{\mathbf{b}, T\mathbf{b}, T^2\mathbf{b}, \ldots\}$.

Definition 4. A *local configuration* (sometimes called a word) $\mathbf{w}$ in a configuration $\mathbf{a} \in A^N$ is a consecutive string of cell states appearing in $\mathbf{a}$ (i.e., a subword of $\mathbf{a}$). We denote the length of the word $\mathbf{w}$ by $|\mathbf{w}|$.

We can enumerate all the words on an infinite lattice according to their length and a prescribed lexicographic order in A.

The cells on a finite periodic lattice of size N are labeled $-[(N-1)/2], \ldots, 0, \ldots, [N/2]$, where the zeroth cell specifies the position of the observer, and $[\cdot]$ is the Gauss symbol. (This should not cause any loss of generality, because the dynamics is translationally invariant.)

Definition 5. A *local configuration around the observer* is a local configuration occupying the cells, $-[(n-1)/2], \ldots, 0, \ldots, [n/2]$. By $[\mathbf{w}]$ we denote the set of all the configurations containing $\mathbf{w}$ as a local configuration around the observer. We call $[\mathbf{w}]$ the *cylinder set around the observer specified by the word* $\mathbf{w}$.

Let $P_{\mathbf{a},N,n}(\mathbf{w})$ be the relative frequency of configurations in $[\mathbf{w}]$ where $\mathbf{w}$ is a local configuration of length n around the observer, in the stationary state $S_{\mathbf{a},N}$; that is,

$$P_{\mathbf{a},N,n}(\mathbf{w}) = \#([\mathbf{w}] \cap S_{\mathbf{a},N}) / \#(S_{\mathbf{a},N}) \tag{A.7}$$

where $\#(*)$ denotes the cardinality of the set $*$. We set

$$P_{\mathbf{a},N,n}(\mathbf{w}) = 0 \tag{A.8}$$

if $|\mathbf{w}| = n > N$. We can define a probability vector whose components are given by $P_{\mathbf{a},N,n}(\mathbf{w})$:

$$\mathbf{P}_{\mathbf{a},N,n} = (P_{\mathbf{a},N,n}(\mathbf{w}_1), \ldots, P_{\mathbf{a},N,n}(\mathbf{w}_M)) \tag{A.9}$$

where $w_1,..., w_M \in A^n$, $M = \#(A^n)$, and the words $w_1,..., w_M$ are ordered lexicographically. We have

$$P_{\mathbf{a},N,n}(b_{-[(n-2)/2]},..., b_0,..., b_{[(n-2)/2]}) = \sum{}' P_{\mathbf{a},N,n}(b_{-[(n-1)/2]},..., b_0,..., b_{[n/2]}) \tag{A.10}$$

where the summation $\sum'$ is over $b_{[n/2]}$ if n is even and $b_{-[n-1/2]}$ if n is odd. This follows from

$$[b_{-[(n-2)/2]},..., b_0,..., b_{[(n-2)/2]}] = \bigcup{}' [b_{-[(n-1)/2]},..., b_0,..., b_{[n/2]}] \tag{A.11}$$

where $\bigcup'$ is over $b_{[n/2]}$ if n is even and $b_{-[(n-1)/2]}$ if n is odd.

Next, we introduce the direct product of $\mathbf{P}_{\mathbf{a},N,n}$ w.r.t. n

$$\mathbf{P}_{\mathbf{a},N} \equiv \prod_{n=0}^{\infty} \mathbf{P}_{\mathbf{a},N,n} \tag{A.12}$$

This is virtually a finite-dimensional vector for finite N due to (A.6). The $\mathbf{P}_{\mathbf{a},N}$ contains all the spatial statistics of the stationary state of the size-N lattice whose initial configuration is $\mathbf{a} \in A^N$.

To take the $N \to \infty$ limit, we must change initial conditions according to the size of the lattice. We specify a sequence of initial conditions as follows. Let $\mathbf{a} \in A^Z$ be

$$\cdots a_{-n} a_{-n+1} \cdots a_0 a_1 \cdots a_n \cdots$$

where $a_i \in A$ for all $i \in Z$. For each $\mathbf{a}$, we make an infinite sequence $\mathscr{P}_{\mathbf{a}}$:

$$\mathscr{P}_{\mathbf{a}} = \{\mathbf{P}_{[\mathbf{a}]_n,n}\}_{n=1}^{\infty} \tag{A.13}$$

where $[\mathbf{a}]_n$ is the local configuration around the observer of length n, which is a word in $\mathbf{a}$. Then we define the totality of $\mathscr{P}_{\mathbf{a}}$ w.r.t. the initial configurations:

$$\mathscr{P} = \bigcup_{\mathbf{a} \in A^Z} \mathscr{P}_{\mathbf{a}} \tag{A.14}$$

$\mathscr{P}_{\mathbf{a}}$ is the totality of the sequence of statistical results for the stationary states of finite-size lattices compatible with the initial configuration $\mathbf{a}$ for an infinite lattice. What we have done above is to collect all the statistical data on the local configurations for larger and larger finite lattices. We expect that the limit in some sense of these statistics gives us the statistical structure of the infinite-lattice limit. More precisely, we expect that the

accumulation points in $\mathscr{P}_{\mathbf{a}}$ are relevant to infinite lattices. To this end we must introduce a metric on $\mathscr{P}$.

We introduce a topology on the set $\mathscr{P}$ through the following compact metric:

$$\|P_{\mathbf{a},N} - P_{\mathbf{b},M}\| \equiv \sum_{n=1}^{\infty} 2^{-n} |\mathbf{P}_{\mathbf{a},N,n} - \mathbf{P}_{\mathbf{b},M,n}| \tag{A.15}$$

where $|\cdot|$ is the usual Euclidean metric, and $\mathbf{P}_{\mathbf{a},N}$, $\mathbf{P}_{\mathbf{b},M} \in \mathscr{P}$. The metric is faithful to our fundamental viewpoint stated at the beginning of Section 4: the factor 2^{-n} accounts for the relative importance of the local configurations close to observer. This factor can be the reciprocal of the nth power of any number larger than 1; any such factor gives the same topology. If $\|P - Q\| = 0$, then all the empirical statistics must be identical for P and Q. However, this does not necessarily imply that $P = Q$, because these vectors are not finite-dimensional. However, the difference between P and Q is not interesting to the localized observer. Therefore, we make the topological space $(\mathscr{P}, \|\cdot\|)$ complete by defining the identity $\approx$ as

$$P \approx Q \Leftrightarrow \|P - Q\| = 0, \qquad \forall P, Q \in \mathscr{P} \tag{A.16}$$

We henceforth identify, for convenience, $\mathscr{P}$ and $\mathscr{P}/\approx$.

The topological space $(\mathscr{P}, \|\cdot\|)$ is sequentially compact. Hence, the set $\mathscr{P}_{\mathbf{a}}$, which is an infinite set, must have an accumulation point for any $\mathbf{a} \in A^Z$. We have the following result.

Proposition. Any accumulation point of $\mathscr{P}_{\mathbf{a}}$ defines a T-invariant σ-additive measure on A^Z.

Proof. Any element of $\mathscr{P}_{\mathbf{a}}$ for finite N, i.e., the vector $\mathbf{P}_{[\mathbf{a}]_N,N}$ defined in (A.5), defines a probability measure $\mu_{\mathbf{a},N}$ on A^N with the consistency condition

$$\mu_{\mathbf{a},N}([\mathbf{w}]) = \sum_{w \backslash w'} \mu_{\mathbf{a},N}([\mathbf{w}]) \tag{A.17}$$

where $\mathbf{w}'$ is a subword of $\mathbf{w}$ and the summation is over all symbols in $w \backslash w'$. This immediately follows from (A.8). This property is inherited by the accumulation points, so any accumulation point of $\mathscr{P}_{\mathbf{a}}$ defines a σ-additive probability measure due to the Kolmogorov existence theorem. By definition, for any N we have

$$\mu_{\mathbf{a},N}(T^{-1}[\mathbf{w}]) = \mu_{\mathbf{a},N}([\mathbf{w}]) \tag{A.18}$$

where T^{-1} is calculated within $S_{\mathbf{a},N}$. Hence, also the accumulation points must have this property, i.e., the measure defined above is T-invariant. ∎

Let us denote the totality of accumulation points $\mathscr{P}_{\mathbf{a}}$ by $\mathscr{Q}_{\mathbf{a}}$ and define

$$\mathscr{Q} = \bigcup_{\mathbf{a} \in A^Z} \mathscr{Q}_{\mathbf{a}} \tag{A.19}$$

Definition 6. A T-invariant measure μ on A^Z defined by any probability vector $\mathbf{P} \in \mathscr{Q}$ is called an invariant measure for the infinite lattice *corresponding to* $\mathbf{P}$.

There may be other invariant measures, which cannot be constructed as above, but since they are inaccessible empirically, we ignore them. $\mathscr{Q}$ or $\mathscr{Q}_{\mathbf{a}}$ can contain many accumulation points. Even for fixed initial condition, different accumulation points may be obtained, e.g., due to the even–odd property of the lattice size.

Definition 7. *Observable invariant measures* are measures corresponding to vectors in $\mathscr{Q}$ that can be reached from ν-positive measure set $\beta \subset A^Z$ of initial conditions, where the measure ν is given by

$$\nu = \lambda \circ s \tag{A.20}$$

with λ being the Lebesgue measure on $[0,1] \times [0,1]$ and $s: A^Z \to [0,1] \times [0,1]$ defined as

$$s(\cdots a_{-m} \cdots a_{-1} a_0 a_1 \cdots a_m \cdots) = \begin{pmatrix} 0 \cdot a_0 a_1 a_2 \cdots a_m \cdots \\ 0 \cdot a_{-1} a_{-2} a_{-3} \cdots a_{-m} \cdots \end{pmatrix} \tag{A.21}$$

where $a_i \in A$ for all $i \in Z$. Here we have assigned consecutive nonnegative integers starting from zero to symbols in the set A and identify the resultant set of nonnegative integers with the original A. The map s is the one that gives, e.g., an isomorphism between a Bernoulli automorphism and the baker's transformation.[26]

ACKNOWLEDGMENTS

We are grateful to E. A. Jackson for valuable comments and critical reading of the manuscript, and to F. Albrecht and O. Martin for useful comments. The work is supported in part by NSF grant DMR-83-16982 through the University of Illinois Materials Research Laboratory.

REFERENCES

1. S. Wolfram, ed., *Theory and Applications of Cellular Automata* (World Scientific, Singapore, 1986).
2. J. Demongeot, E. Cole, and M. Tchuente, eds., *Dynamical Systems and Cellular Automata* (Academic Press, New York, 1985).
3. K. Kaneko, *Prog. Theor. Phys.* **72**:480 (1984); R. J. Deissler, *Phys. Lett.* **100A**:451 (1984); R. Kapral, *Phys. Rev. A* **32**:1076 (1985).
4. Y. Oono and M. Kohmoto, *Phys. Rev. Lett.* **55**:2927 (1985).
5. D. Ruelle, *Thermodynamic Formalism* (Benjamin, New York, 1978).
6. D. Ruelle and F. Takens, *Commun. Math. Phys.* **20**:167 (1971); **23**:343 (1971); S. Newhouse, D. Ruelle, and F. Takens, *Commun. Math. Phys.* **64**:35 (1978).
7. J. B. McLaughlin and P. C. Martin, *Phys. Rev. A* **12**:186 (1975).
8. E. N. Lorenz, *J. Atmos. Sci.* **20**:130 (1963).
9. T. Y. Li and J. A. Yorke, *Am. Math. Month.* **82**:985 (1975).
10. R. M. May, *Nature* **261**:459 (1976).
11. D. Ruelle, *Commun. Math. Phys.* **93**:285 (1984); P. Constantine and C. Foias, *Commun. Pure Appl. Math.* **38**:1 (1985).
12. A. R. Bishop, K. Fesser, P. S. Lomdahl, W. C. Kerr, M. B. William, D. F. Dubois, H. A. Rose, and B. Hafizi, *Phys. Rev. Lett.* **51**:335 (1983); A. R. Bishop, K. Fesser, and D. S. Lomdahl, *Physica* **7D**:259 (1983).
13. Y. Oono, *Prog. Theor. Phys.* **60**:1583 (1979).
14. Y. Oono and M. Osikawa, *Prog. Theor. Phys.* **64**:1804 (1980); M. Osikawa and Y. Oono, *Publ. RIMS (Kyoto Univ.)* **17**:165 (1981).
15. J. Guckenheimer, *Commun. Math. Phys.* **70**:133 (1979).
16. A. K. Zvonkin and L. A. Levin, *Russ. Math. Surv.* **25**(6):83 (1970).
17. J. Ford, in *Long-Time Prediction in Dynamics*, C. W. Horton, Jr., L. E. Reichl, and V. G. Szebehely, eds. (Wiley, New York, 1982).
18. A. A. Brudno, *Trans. Moscow Math. Soc.* **44**:127 (1983).
19. S. Wolfram, *Physica* **10D**:35 (1984); in *Theory and Applications of Cellular Automata*, S. Wolfram, ed. (World Scientific, Singapore, 1986).
20. N. Packard, in *Dynamical Systems and Cellular Automata*, J. Demongeot, E. Cole, and M. Tchuente, eds. (Academic Press, New York, 1985).
21. U. Frisch, B. Hasslacher, and Y. Pomeau, *Phys. Rev. Lett.* **56**:1505 (1986).
22. Y. Oono and S. Puri, *Phys. Rev. Lett.* **58**:836 (1987); R. Kapral and G. L. Oppo, preprint (1986).
23. Y. Takahashi and Y. Oono, *Prog. Theor. Phys.* **71**:851 (1984).
24. S. Willson, *Math. Systems Theor.* **9**:132 (1975).
25. M. Miyamoto, *J. Math. Kyoto Univ.* **19**:525 (1979).
26. P. Walters, *An Introduction to Ergodic Theory* (Springer, New York, 1982).
27. Y. Kuramoto, *Chemical Oscillation, Waves and Turbulence* (Springer, New York, 1984).
28. N. Koppel, in *Proceedings of the International Congress of Mathematicians*, Vol. 2, Section 18, Z. Ciesielski and C. Olech, eds. (Polish Scientific Publishers, Warsaw, 1984).
29. Y. Kuramoto and T. Yamada, *Prog. Theor. Phys.* **56**:679 (1976); T. Yamada and Y. Kuramoto, *Prog. Theor. Phys.* **56**:681 (1976); Y. Kuramoto, *Prog. Theor. Phys. Suppl.* **64**:346 (1978); see also Y. Kuramoto, *Prog. Theor. Phys.* **63**:1885 (1980).
30. G. J. Sivashinsky, *Acta Astronaut.* **4**:1177 (1977).
31. H. Yamazaki, Y. Oono, and K. Hirakawa, *J. Phys. Soc. Jpn.* **44**:335 (1978); H. Yamazaki, Y. Oono, and K. Hirakawa, *J. Phys. Soc. Jpn.* **46**:721 (1979).
32. J. J. Tyson, in *The Belousov–Zhabotinsky Reaction*, S. Levine, ed. (Springer, Berlin, 1976).

33. M. Fujisaka and T. Yamada, *Z. Phys.* **28B**:239 (1977).
34. T. Niwa, *J. Stat. Phys.* **18**:3 (1978).
35. Y. Oono, T. Kohda, and H. Yamazaki, *J. Phys. Soc. Jpn.* **48**:738 (1980).
36. T. Winfree, *Sci. Am.* **230**:82 (1974).
37. F. Madore and W. L. Freeman, *Science* **222**:615 (1983).
38. P. Grassberger, F. Krause, and T. von der Twen, *J. Phys. A* **17**:L105 (1984).
39. S. Smale, *Bull. Am. Math. Soc.* **73**:747 (1967); R. Bowen, *On Axiom A Diffeomorphisms* (AMS, Providence, Rhode Island, 1977).
40. J. Milnor and W. Thurston, On Iterated Maps of the Interval I, II, mimeographed note Princeton (1977); Y. Takahashi, *Osaka J. Math.* **20**:599 (1983).
41. M. Loeve, *Probability Theory I* (Springer, New York, 1977), Section 4.3.
42. D. S. Ornstein, *Ergodic Theory, Randomness and Dynamical Systems* (Yale University, New Haven, 1984).
43. M. Aizenmann, S. Goldstein, and J. L. Lebowitz, *Commun. Math. Phys.* **39**:289 (1975).
44. Ya. Sinai, *Sov. Math. Dokl.* **4**:1818 (1963).
45. S. Kalikow, *Ann. Math.* **115**:398 (1982).
46. M. Davis, *Computability and Unsolvability* (Dover, New York, 1982).
47. P. Billingsley, *Ergodic Theory and Information* (Wiley, New York, 1965).
48. W. Krieger, *Trans. Am. Math. Soc.* **149**:453 (1970); Erratum **168**:519 (1972).
49. O. Martin, A. Odlyzko, and S. Wolfram, *Physica* **10D**:219 (1984).